A Database of Cepheid Distance Moduli and TRGB, GCLF, PNLF and SBF Data Useful for Distance Determinations

Accepted for publication in the *Astrophysical Journal Supplement Series*

Laura Ferrarese[1,2] Holland C. Ford[3], John Huchra[4], Robert C. Kennicutt, Jr.[5], Jeremy R. Mould[6], Shoko Sakai[7] Wendy L. Freedman[8], Peter B. Stetson[9], Barry F. Madore[10], Brad K. Gibson[11], John A. Graham[12], Shaun M. Hughes[13], Garth D. Illingworth[14], Daniel D. Kelson[12], Lucas Macri[4], Kim Sebo[6] & N.A. Silbermann[10]

ABSTRACT

We present a compilation of Cepheid distance moduli and data for four secondary distance indicators that employ stars in the old stellar populations: the planetary nebula luminosity function (PNLF), the globular cluster luminosity function (GCLF), the tip of the red giant branch (TRGB), and the surface brightness fluctuation (SBF) method. The database includes all data published as of July 15, 1999. The main strength of this compilation resides in all data being on a *consistent and homogeneous* system: all Cepheid distances are derived using the same calibration of the period-luminosity relation, the treatment of errors is consistent for all indicators, measurements which are not considered reliable are excluded. As such, the database is ideal for inter-comparing any of the distance indicators considered, or for deriving a Cepheid calibration to any secondary distance indicator, such as the Tully-Fisher

[1]Hubble Fellow

[2]California Institute of Technology, Pasadena CA 91125, USA

[3]Johns Hopkins University and Space Telescope Science Institute, Baltimore MD 21218, USA

[4]Harvard Smithsonian Center for Astrophysics, Cambridge MA 02138 USA

[5]Steward Observatories, University of Arizona, Tucson AZ 85721, USA

[6]Research School of Astronomy & Astrophysics, Institute of Advanced Studies, ANU, ACT 2611, Australia

[7]Kitt Peak National Observatory, NOAO, Tucson AZ 85726, USA

[8]Carnegie Observatories, Pasadena CA 91101, USA

[9]Dominion Astrophysical Observatory, Victoria, British Columbia V8X 4M6, Canada

[10]NASA/IPAC Extragalactic Database and California Institute of Technology, Pasadena CA 91125, USA

[11]CASA, University of Colorado, Boulder, CO, USA

[12]Department of Terrestrial Magnetism, Carnegie Institution of Washington, Washington DC 20015, USA

[13]Royal Greenwich Observatory, Cambridge CB3 OHA, UK

[14]Lick Observatory, University of California, Santa Cruz CA 95064 USA

relation, the Type Ia Supernovae, or the fundamental plane for elliptical galaxies. This task has already been undertaken by Ferrarese et al. (2000a), Sakai et al. (2000), Kelson et al. (2000) and Gibson et al. (2000). Specifically, the database includes: 1) Cepheid distances, extinctions and metallicities; 2) reddened apparent λ5007 Å magnitudes of the PNLF cutoff; 3) reddened, apparent magnitudes and colors of the turnover of the GCLF (both in the $V-$ and $B-$bands); 4) reddened, apparent magnitudes of the TRGB (in the $I-$band) and $V-I$ colors at and 0.5 magnitudes fainter than the TRGB; 5) reddened, apparent surface brightness fluctuation magnitudes measured in Kron-Cousin I, K', K_{short}, and using the F814W filter with the HST/WFPC2. In addition, for every galaxy in the database we give reddening estimates from DIRBE/IRAS as well as HI maps, J2000 coordinates, Hubble and T-type morphological classification, apparent total magnitude in B, and systemic velocity.

1. Introduction

The Hubble Space Telescope (HST) Key Project on the Extragalactic Distance Scale (Kennicutt, Freedman & Mould 1995, Ferrarese et al. 1999) as well as other HST programs (Saha et al. 1995, 1996a, 1996b, 1997, 1999, Tanvir et al. 1995), have provided Cepheid distances to 24 galaxies in 11 clusters as far as Virgo and Fornax. Added to the existing ground-based Cepheid distances to 10 Local Group galaxies, they constitute a solid background against which to calibrate secondary distance indicators. To do so, the first step is to collect the available data, which are often inhomogeneous in terms of adopted zero point, extinction correction, and error analysis, and set them on a common scale. In this paper we accomplish this task for the published Cepheid distances as well as for four distance indicators that employ stars in the old stellar populations (Pop II): the tip of the red giant branch (TRGB), the planetary nebula luminosity function (PNLF), the globular clusters luminosity function (GCLF) and the surface brightness fluctuation method (SBF). All data available in the literature as of July 15, 1999 are reviewed. While this paper deals exclusively with the issue of compiling a homogeneous database, a second paper (Ferrarese et al. 2000a) uses the database to provide a Cepheid based calibration for the above-mentioned distance indicators, and employs SBF distances to step out into the Hubble flow and derive a value for the Hubble constant.

Extensive reviews of the TRGB, PNLF, GCLF and SBF, and their application as distance indicators have been published by Madore et al. (1996), Sakai (1999), Jacoby et al. (1992), Jacoby (1996), Jacoby (1998), Whitmore (1996), Tonry et al. (1996) and Blakeslee, Ajhar & Tonry (1998). All methods are also reviewed critically in Ferrarese et al. (2000a), where relative strengths and weaknesses are discussed. This paper is organized as follows. The next sections will describe the database (§2), outline the criteria used in homogenizing the published data and discuss cases that needed special attention (§3 to §7). Relative distances to galaxies in groups and clusters allow

the study of the clusters' geometry. Furthermore, a Cepheid calibration or a comparative study of any secondary distance indicators can be accomplished either by using a direct comparison or group mean distances. Therefore we discuss the group/cluster membership for every galaxy in the database in Appendix A.

2. Description of the Database

The task of compiling an internally consistent database is achieved by 1) assuring that Cepheid distance moduli share the same calibration and a common procedure in fitting the period-luminosity (PL) relation; 2) publishing reddened, characteristic magnitudes rather than distance moduli for the TRGB, PNLF, GCLF and SBF methods: listed in the database are the $I-$band magnitudes of the TRGB, I_{TRGB}, the cutoff magnitude of the PNLF, m^* (measured in the [OIII]λ5007 emission), the turnover magnitude of the GCLF, m_T, and the fluctuation magnitude for SBF, $\overline{m}$, all of which are not corrected for Galactic reddening; 3) considering a consistent error analysis for each indicator.

We review all Cepheid distance moduli, and all TRGB, PNLF, GCLF, and SBF data published in refereed journals as of July 15, 1999. In some cases, slight changes to the published data were necessary to conform to the criteria given above, these cases are discussed in §3 through §7. The $I-$band SBF (hereafter I-SBF) dataset of Ajhar et al. (1999), is finalized but not yet published at the time this paper is written, and it has not been duplicated here in its entirety. Rather, we include in this paper only I-SBF fluctuation magnitudes to galaxies with at least one other Cepheid, TRGB, GCLF or PNLF measurement. Reddening corrected and calibrated PNLF, GCLF, SBF and TRGB distance moduli for all galaxies considered in this paper can be found in Ferrarese et al. (2000a).

The database consists of three tables. Table 1 gives general information for all galaxies with at least one Cepheid, TRGB, PNLF, GCLF, or SBF measurement (with the above-mentioned exception of the I-SBF database of Ajhar et al.). The table is organized as follows: Column 1: galaxy name; columns 2 and 3: right ascension and declination at J2000; columns 4 and 5: Hubble Type and T-type respectively; column 6: total apparent B magnitude, B_T; column 7: heliocentric systemic velocity (in km s^{-1}). All entries are from the RC3 (de Vaucouleurs et al. 1991) except for the heliocentric velocity, which is taken from various sources as listed by the NASA Extragalactic Database (NED). The galaxies are organized in order of increasing right ascension.

For the same galaxies listed in Table 1, Table 2 includes reddening and metallicity indicators appropriate to the stellar population employed by each method. Three reddening estimates are given: the total (Galactic plus internal) reddening determined from observations of Cepheids (when available) in column 2; the Galactic reddening based on the DIRBE/IRAS maps of Schlegel et al. (1998) in column 3; the Galactic reddening based on the HI maps of Burstein & Heiles (1984) in column 4. From the data listed in the table, reddening

correction can be performed easily once an extinction curve is adopted: for example, for $R_V = 3.3$, the extinction curves of Cardelli, Clayton & Mathis (1989) give the following ratios for the absorption: $A(B) : A(5007) : A(V) : A(I) : A(F814W) : A(K_s) : A(K') =$ 1.288:1.120:1:0.600:0.596:0.120:0.125. The metallicity indicators listed in Table 2 are as follows: the metallicity for the old stellar population in elliptical galaxies and bulges is measured by the Mg_2 indexes (column 5) and by the $V - I$ colors determined in parallel to the SBF measurements (column 10); globular cluster metallicities are represented by the globular cluster color determined at a turnover magnitude of the GCLF (column 6); the Cepheid metallicity is given in column 7 as the [O/H] index for the HII regions in the immediate vicinity of the Cepheids; finally the metallicity of the halo can be estimated from the $V - I$ colors determined at the TRGB (column 8), or more precisely at an absolute I magnitude of ~ -3.5, or 0.5 magnitudes fainter than the TRGB (column 9). References are given in the notes to the table.

Cepheid distance moduli and magnitudes for the secondary distance indicators are listed in Table 3. Here, the galaxies are organized according to group membership, as defined in Appendix A. The columns are as follows. (1): galaxy name; (2), (3), (4) and (5): the number of Cepheids used in determining the PL relation, the photometric bands in which the Cepheid observations were carried out, the Cepheid distance modulus and references respectively; (6) and (7) the apparent I magnitude of the TRGB not corrected for Galactic extinction, and references; (8), (9) and (10): the number of PNe used in fitting the PNLF, the apparent PNLF cutoff magnitude, uncorrected for extinction, and references; (11) and (12): the apparent turnover magnitude of the GCLF, uncorrected for extinction and determined in the photometric band listed next to each measurement, and references; (13) and (14): the SBF fluctuation magnitude, uncorrected for extinction, and determined in the photometric band listed next to each measurement, and references. When quoting data from this paper, the references given in the table should be cited.

In Tables 2 and 3, data followed by a colon are reported for completeness, but not considered reliable for the purpose of calibrating the distance indicators, for the reasons outlined in the following sections.

3. Cepheid Distances

Table 3 lists published Cepheid distances. When multiple measurements to the same galaxy exist, we only list the most comprehensive (and generally most recent) study.

To insure homogeneity within the sample, it is necessary that: a) all Cepheid distances rely on the same absolute calibration, i.e. adopt a common zero point and slope for the period-luminosity (PL) relation; b) possible incompleteness biases affecting the PL relation are taken into account; c) extinction corrections are performed according to a common reddening law and the same value of the ratio of total to selective absorption R_V; and d) a common and complete list of uncertainties is factored in when calculating the error in the quoted distances.

The PL calibration adopted in this paper is based on a sample of 32 LMC Cepheids with BVI photoelectric photometry and periods in the range from 1.5 to 63 days (Madore & Freedman 1991). The absolute calibration assumes a true distance modulus and average line-of-sight reddening to the LMC of 18.50 ± 0.13 mag (Mould et al. 2000) and $E(B-V) = 0.10$ mag respectively, a ratio of total to selective absorption $R_V = A(V)/E(B-V) = 3.3$, and a reddening law following Cardelli, Clayton and Mathis (1989). This calibration is shared by all but two of the published Cepheid distances. The exceptions are the Small Magellanic Cloud (Welch et al. 1987) and NGC 3109 (Musella et al. 1997), and are discussed in §3.2 and §3.3.

In their discussion of the distance modulus to the Virgo cluster galaxy M100, Ferrarese et al. (1996) performed a detailed analysis of the bias arising from magnitude incompleteness at short periods. It was concluded that the Cepheid sample in M100 is substantially incomplete below 20 days. Because of the finite width of the Cepheid PL relation, only the brighter Cepheids are recovered at the faint end of the PL relation, leading to an underestimate of the distances by 0.05-0.10 magnitudes if the bias is not corrected. These conclusions are further supported by artificial star tests to be discussed in Ferrarese et al. (2000b). At the distance modulus of the Virgo and Fornax clusters, these tests show that the V PL relation is $\sim$50% incomplete below $20-25$ days. Because of these results, we found it necessary to revisit the HST Cepheid distances published as part of the Key Project. For each galaxy we calculated distance moduli for samples with different lower cutoff in period. In a few cases (NGC 1365, NGC 1326A, NGC 1425, NGC 4725 and NGC 4535) we found that the distance modulus increases when the lower period cutoff is moved from ~ 10 to $\sim 20-25$ days, the exact period depending on the distance and level of crowding in the galaxy. The period cutoff above which the distance moduli stabilize is then applied to the data. This produces an increase in the derived distance modulus of ~ 0.1 mag at most. Changes made to published distance moduli are detailed in Table 4. Notice that a lower period cutoff was not applied to the LMC Cepheid sample that calibrates the PL relation, however, because the slope of the PL relation fitted to each distant galaxy is kept fixed to the LMC value, this does not introduce a bias in the derived distance moduli (e.g., Graham et al. 1999).

To allow for meaningful weighting, all published error estimates have been revised slightly to include only random contributions. A typical example of the error budget adopted is presented in Ferrarese et al. (2000a). Random sources of error include scatter in the fit of the PL relation, and the error on the assumed value of the ratio of total to selective absorption, R_V. Systematic sources of error include the uncertainty in the distance to the LMC and the error in the zero point of the LMC PL relation. For the Cepheid distances based on HST photometry, we have treated the photometric error as systematic, rather than random; therefore the sum, in quadrature, of all of the above systematic errors, amounts to 0.16 mag, and has not been listed explicitly in Table 3. For the Cepheid galaxies based on ground-based photometry, the only sources of systematic error are the uncertainty in the LMC distance and the LMC PL relation zero point, 0.13 magnitudes; the photometric errors have been treated as random. It follows that if a sample of Cepheid is used including *both* ground-based and HST observations, a 0.14 mag uncertainty (due to photometric

zero points errors) must be added in quadrature to the error reported in Table 3 for the *HST* galaxies, and the systematic error for the entire sample would be reduced to 0.13 mag.

Distance uncertainties arising from a possible metallicity dependence of the Cepheid PL relation (e.g. Kennicutt et al. 1998) are not accounted for at this stage. Metallicity effects on the calibration of secondary distance indicators are considered explicitly in Ferrarese et al. (2000a), Sakai et al. (2000), Kelson et al. (2000), and Gibson et al. (2000).

The reddening derived from multi-wavelength observations of Cepheids is listed in column 2 of Table 2 as $E(B-V) = A_V/3.3 = 0.742 \times E(V-I)$. Errors are associated with the reddening only when given by the authors. If Cepheids are observed in only one photometric band, a N/A appears in column 2. Note that $E(B-V)$ includes both foreground (Galactic) and internal extinction, and should therefore be larger than the Schlegel et al. (1998) and Burstein & Heiles (1984) $E(B-V)$ values given in columns 3 and 4 of Table 2.

3.1. Rejected Cepheid Distances

Sandage & Carlson (1985) published periods and light curves for 15 Cepheids in the WLM galaxy. Their photometry was subsequently questioned by Ferraro et al. (1989); furthermore, all of the WLM Cepheids have periods less than 10 days, and might therefore be contaminated by overtone pulsators. Therefore we do not include the WLM distance in the database.

Cepheid distances based on observations in a single photometric band are listed in the database as upper limits, because of the impossibility of deriving a mean internal reddening (Freedman & Madore 1988). These galaxies include Holmberg II (=UGC 4305), NGC 2403, GR8, NGC 2366 and NGC 4571.

3.2. Cepheid Distance to the Small Magellanic Cloud

Preceding the Madore & Freedman PL calibration, Welch et al. (1987) derived $(m-M)_{SMC} = 18.93 \pm 0.05$ mag and negligible extinction for the Small Magellanic Cloud, from HJK photometry of 91 Cepheids. Using the same data, and adopting zero points and slopes derived for the IR PL relations by Madore and Freedman (1991), we obtain apparent distance moduli $(m-M)_J = 18.997 \pm 0.024$, $(m-M)_H = 19.013 \pm 0.022$, and $(m-M)_K = 18.989 \pm 0.022$, where the errors reflect only the rms scatter around the mean PL relation. Using the Cardelli, Clayton and Mathis (1989) reddening law with $R_V = 3.3$, the true distance modulus and reddening to the SMC are $(m-M) = 18.99 \pm 0.05$ and $E(B-V) = 0.01 \pm 0.05$. The error on the distance modulus accounts for a 3% error in the photometry (Welch et al. 1987), the scatter in the PL relations, and the (negligible) error in the assumed value of R_V.

3.3. Cepheid Distance to NGC 3109

The most recent and complete data set for Cepheid variables in NGC 3109 were presented by Musella, Piotto & Capaccioli (1997). Sixteen of their 36 Cepheids (with periods in the range 2.8 to 20 days) have $BVRI$ measurements. A distance modulus $(m-M) = 25.67 \pm 0.16$, and reddening $E(B-V) = -0.01 \pm 0.04$ are derived using a calibrating PL relation based on Sandage (1988) and Madore & Freedman (1991), and distance modulus and reddening for the LMC of 18.50 mag and $E(B-V) = 0.08$ mag respectively.

We derived a distance to NGC 3109 by applying the standard procedure described in §3. We therefore selected only Cepheids with period larger than 10 days and observed in all available passbands, $BVRI$. Unfortunately, this reduces the sample to only four Cepheids, with the consequence that the distance cannot be constrained too well. The exclusion of short period Cepheids is necessary in order to avoid overtone pulsators and the possibility of magnitude incompleteness: from Figures 4−7 of Musella et al. , Cepheids with periods shorter than 10 days clearly define a brighter PL relation than Cepheids with longer period. Our procedure yields apparent distance moduli $(m-M)_B = 25.97 \pm 0.18$, $(m-M)_V = 25.91 \pm 0.14$, $(m-M)_R = 25.71 \pm 0.11$, and $(m-M)_I = 25.60 \pm 0.09$. From this we obtain a formal true distance modulus $(m-M) = 25.26 \pm 0.22$ mag, and a reddening $E(B-V) = 0.18 \pm 0.08$ mag. This result is obtained by using weights proportional to the inverse square of the errors on the individual apparent distance moduli, not using weights would increase the distance modulus by 0.05 mag. In the particular case of NGC 3109, for which most of the observed Cepheids are at short period, a better estimate of the reddening could be obtained by calculating the reddening for all of the Cepheids on an individual basis, rather than for the combined long period subset. This procedure is however not standard for the galaxies observed by the Key Project and would introduce inhomogeneities. The adoption of a different PL calibration, and the exclusion of short period Cepheids contribute in equal amount to the difference between our distance and Musella et al.

4. Tip of the Red Giant Branch Distances

For distance determinations, the magnitude of the TRGB is always measured in the $I-$band, since this is where metallicity effects are minimized (Lee, Freedman & Madore 1993). Metallicity corrections can be estimated from the $V-I$ color at the TRGB and 0.5 mag fainter (corresponding roughly to an absolute magnitude $M_I = -3.5$). These, uncorrected for foreground extinction, are listed in columns 8 and 9 of Table 2, with the exception of NGC 3379 (Sakai et al. 1997), and IC 3388 (Harris et al. 1998), for which only I data were obtained.

The TRGB I_{TRGB} magnitude (uncorrected for extinction) and associated error are listed in column 6 of Table 3. Most authors include the internal uncertainty of the fit to the TRGB in the error quoted for I_{TRGB}, and incorporate photometric errors in the final distance modulus.

Therefore, to obtain a consistent dataset, photometric errors (as quoted by the authors) and uncertainties in the TRGB fit were added in quadrature to produce the I_{TRGB} error listed in Table 3.

5. Planetary Nebulae Distances

The λ5007 Å cutoff magnitude of the PNLF, m^*, uncorrected for foreground extinction, is listed in column 9 of Table 3. Because PNLF distance moduli are calculated by fitting the luminosity function with a standard template (e.g. Ciardullo et al. 1989), only the final distance moduli are published. From these we derived m^* *a posteriori* by subtracting the zero point (and the extinction correction if applied) adopted by the authors. The PNLF distances to the SMC, NGC 3109, and NGC 5253, listed in Table 3, are not well constrained. The PNe sample in NGC 3109 (Richer & McCall 1992) includes only seven objects, and an upper limit to the distance is derived from the brightest of the PNe observed. Jacoby, Walker & Ciardullo (1990) advise against the use of the PNLF distance to the SMC due to the small number of PNe defining the luminosity function. Finally, the small number of PNe detected in NGC5253, the presence of strong internal dust extinction, and the galaxy's very low metal abundance all conjure to produce a very ill constrained PNLF magnitude cutoff, unsuitable for distance determinations (Phillips et al. 1992).

Uncertainties in the values of m^* are summarized, for example, in Jacoby, Ciardullo & Ford (1990). They include a contribution associated with the fitting procedure (of the order of 0.10 mag), photometric zero points ($\sim$ 0.05 mag), the filter response calibration ($\sim$ 0.04 mag), and the uncertain definition of the empirical PNLF ($\sim$ 0.05 mag). Errors in the reddening estimate, which are sometimes included, have been removed (in quadrature) from the present analysis, as we only deal with uncorrected magnitudes.

6. Globular Clusters Luminosity Function Distances

The task of building a homogeneous data sample from the available GCLF data is far from simple. Most of the published data are in the $V-$band, or in the C, T_1 Washington system which can readily be transformed to give V magnitudes (Geisler 1996). However, there are several cases in which only the $B-$band luminosity function is presented.

The turnover magnitude cannot be properly estimated unless the luminosity function extends beyond it (Ferrarese et al. 2000a); galaxies with a GCLF not sampling the turnover are therefore not included in our database. Unfortunately, this excluded NGC 720 (Kissler-Patig et al. 1996), NGC 4636 (Kissler et al. 1994), the Fornax sample of Kohle et al. (1996), the Virgo cluster sample of Ajhar et al. (1994), NGC 1400 and NGC 1407 in the Eridanus cluster (Perrett et al. 1997), and NGC 4881 in Coma (Baum et al. 1995). The GCLF for NGC 1399 published by Bridges, Hanes & Harris (1991) presented us with a difficult choice. The authors fit the V GCLF using fixed σ

in the range $1.00 \leq \sigma \leq 1.75$ and find that χ^2 is minimized for $\sigma \sim 1.5$, giving a turnover at $V = 24.10$, only 0.3 magnitudes fainter than their magnitude limit. In B, however, the χ^2 of the fit keeps decreasing while sigma is increased, up to the last fitted value of $\sigma = 1.75$, which gives a turnover half a magnitude fainter than the magnitude cutoff of the data. There are not enough data in the literature to determine whether the GCLF dispersion in B is intrinsically larger than in V, and therefore to decide whether the Bridges et al. results are simply due to the B data being more incomplete than (not as deep as) the V data, or to the fact that the turnover magnitude is not sampled well enough to determine an accurate distance. For these reasons, we conservatively excluded the Bridges et al. data from our sample. Finally, the Elson & Santiago (1996) study of globular clusters in M87 was not considered because the authors warn that the difficulty in estimating the contamination from background galaxies makes the determination of the turnover magnitude very uncertain and not suitable for distance determinations.

Four cases required further attention. The NGC 3031 data of Perelmuter & Racine (1995) do extend beyond the turnover, but the procedure used to analyze the data is unclear. We could not determine whether the authors solved for σ or not. We performed a three parameter Gaussian fit to the data, and found $V = 20.86 \pm 0.46$ and $\sigma = 1.46 \pm 0.25$. This is significantly different from the published value of $V = 20.3 \pm 0.3$. The source of this difference is unclear, and the data have large errorbars; consequently, we decided to exclude the GCLF distance to NGC 3031 from our sample.

In the case of NGC 3377, Harris (1990) found it necessary to combine the GCLF with that of NGC 3379, assumed to be at the same distance. This produces a sufficiently well defined GCLF for a three parameter fit. We found that a three parameter fit to the NGC 3377 GCLF alone is possible even if rather shaky. Our fit gives $B = 23.13 \pm 0.32$ and $\sigma = 0.88 \pm 0.22$ for NGC 3377, in reasonably good agreement with the Harris values of $B = 23.35 \pm 0.40$ for the combined NGC 3377 + NGC 3379 GCLF. However, we follow Harris' conclusion that a fit to NGC 3377 alone is not reliable, and we do not include this measurement in our table.

We also performed our own fit to the Fleming et al. (1995) data for NGC 4494. In spite of the fact that the GCLF does sample the turnover, the authors fixed the value of σ in fitting the data. We found $V = 23.32 \pm 0.35$ and $\sigma = 1.31 \pm 0.18$, and adopt it in our Table 3. This compares to the published $V = 23.6 \pm 0.4$, which assumes a σ of 1.4.

Finally, for IC 4051 in Coma, we quote in Table 3 the best fit to the turnover reported by Baum et al. (1997) using a Gaussian fit. The authors do not give an error for this measurement; consequently, we adopted half the difference between the turnover magnitudes obtained by Baum et al. by fitting a Gaussian and an asymmetric hyperbolic function as an estimate of the uncertainty. It is not entirely clear whether the dispersion of the Gaussian was allowed to vary in the fit, and we cannot reproduce the result because the data are not tabulated.

In keeping with our precepts, the GC data reported in Tables 2 and 3 are not corrected for either internal or Galactic reddening. The turnover magnitudes are listed in column 11 of

Table 3, and the GC color at the turnover, when available, can be found in column 6 of Table 2. Photometric errors are always small compared to the formal uncertainty in the Gaussian fits to the GCLF, and have not therefore been taken into account: the quoted errors for the turnover magnitudes in Table 3 include only the formal uncertainty in the fit. There are, of course, exceptions. *HST* data often comprise large samples of GCs extending well beyond the turnover of the luminosity function, and the fits are very well constrained. Therefore, we added (in quadrature) a 0.06 magnitude uncertainty to the fitting error quoted for NGC 1399, NGC 1404, NGC 3113, NGC 4486, NGC 5846, NGC 4494 and NGC 4278 (Grillmair et al. 1999, Kundu & Whitmore 1998, Forbes 1996a, Forbes et al. 1997, Kundu et al. 1998). This accounts for a 0.05 mag error in the photometric zero point, plus a 0.03 magnitude error in the photometric aperture correction (Holtzman et al. 1995).

A final note of caution is necessary. Measuring the peak of GCLFs is very tricky: it requires precise estimates of 1) the incompleteness of the data, 2) the errors as a function of magnitude (that will 'scatter' points preferentially to brighter magnitudes), and 3) the contribution of the background galaxy population. In the worse case, all these effects can induce a 0.5 magnitude error if not taken into account. We did not attempt to quantify or check any of these effects; instead we rely on the authors' analysis.

7. Surface Brightness Fluctuation Distances

The surface brightness fluctuation method has been employed in ground based surveys using the Kron-Cousins $I-$band (Ajhar et al. 1999) and the near-infrared K' ($\lambda_c = 2.10\mu$m) and K_s ($\lambda_c = 2.16\mu$m) filters (Jensen et al. 1996, Pahre & Mould 1994). Several galaxies have been observed with the F814W filter using the *HST*/WFPC2 (Ajhar et al. 1997, Lauer et al. 1998). Because of the dependence of the fluctuation magnitude on the stellar population, SBF observations in different passbands are listed separately in Table 3 (column 13). All fluctuation magnitudes include a $k-$correction term, but are not extinction corrected. Errors on the quoted magnitudes and colors include photometric zero points errors, and the estimated error on the fluctuation magnitudes.

The calibration of the SBF method includes a strong metallicity dependence (Tonry et al. 1997), which can be quantified through the mean $V - I$ color of the region in which the fluctuations are determined. This is listed in column 10 of Table 2, also uncorrected for extinction, but including a $k-$correction term.

8. Summary

We have presented a homogeneous compilation of Cepheid, TRGB, PNLF, GCLF and SBF data that can be used in determining distances to external galaxies. The database represents the

most complete and coherent collection of measurements for both the Cepheids and the four Pop II distance indicators as of July 15, 1999. All data, with the exception of the Cepheid distance moduli, are uncorrected for Galactic extinction, estimates of which are given based both on DIRBE/IRAS maps (Schlegel et al. 1998) and HI maps (Burstein & Heiles 1984). Reddening corrected distance moduli are given for all of the galaxies in the database in Ferrarese et al. (2000a), using a calibration based on Cepheids. Cepheid distances presented in this paper have also been used for the calibration of the Tully-Fisher relation (Sakai et al. 2000), Type Ia supernovae (Gibson et al. 2000), and the fundamental plane of elliptical galaxies (Kelson et al. 2000)

We wish to thank John Tonry, John Blakeslee, Ed Ajhar and Alan Dresser for kindly giving us access to the SBF database prior to publication. LF acknowledges support by NASA through Hubble Fellowship grant HF-01081.01-96A awarded by the Space Telescope Science Institute, which is operated by the Association of Universities for Research in Astronomy, Inc., for NASA under contract NAS 5-26555. Support for this work was also provided by NASA through grant GO-2227-87A from STScI. This research has made use of the NASA/IPAC Extragalactic Database (NED), version 2.5 (May 27, 1998). NED is operated by the Jet Propulsion Laboratory, California Institute of Technology, under contract with the National Aeronautics and Space Administration.

A. Identification of Groups and Cluster

A complete compilation of galaxies belonging to different groups and clusters is beyond the scope of this paper. Our goal is to establish physical associations between galaxies with a measured Cepheid distance and at least one between PNLF, GCLF, TRGB, and SBF distance estimates. Group membership for all of the galaxies of interest has been analyzed using the CfA redshift catalogue (zcat, version July 1998, Huchra & Mader 1998). Criteria for group membership vary from group to group: a detailed description of the methodology adopted is given below for each case. When possible, our analysis has been supplemented with published studies of galaxy groups, as listed below. For each identified group, galaxies are divided into three classes: certain members (galaxies for which group membership is beyond any doubt, based on position, redshift and, when available, previous population studies of the group), probable members (galaxies that are most likely true members, but are slightly too far, in either space or redshift, from the certain members of the group to pass the 'beyond any reasonable doubt' condition, according to criteria established below for each group), and possible members (galaxies that are probably not true members, but for which the association with the group cannot be completely excluded). Finding charts for all galaxies in each group are given in Figures 1a and 1b, and cluster properties are given in Table 5.

The M81 Group. An inspection of zcat shows that the galaxies in the M81 group are divided in two separate sub-clumps: the first extends in a $4^\circ \times 2^\circ$ region centered on M81, while the second is located about 13° to the east. The core of the group, defined by M81, NGC 3034 and NGC 3077, is very compact: the three galaxies are found within 1° and 100 km s^{-1} of each other. IC 2574 and

NGC 2976 are located 2° to 3° from M81, and have comparable velocity. The second sub-clump, 13° to the east of M81, is defined by NGC 2366, NGC 2403, and 08141+7052. In view of the fact that all the galaxies in the two sub-clumps share the same systemic velocity within 400 km s^{-1}, we classify NGC 2366 and NGC 2403 as probable members of the M81 group, in spite of the large separation from the galaxies defining the group core. NGC 2787 is located 3.°3 west of M81. The systemic velocity of 700 km s^{-1} places it at the high boundary of the velocity distribution for the M81 group, and therefore we classify this galaxy as a possible member. In the Nearby Galaxies Catalog (Tully 1988, hereafter T88), M81, NGC 3077, NGC 2403 and NGC 2366 are all identified as belonging to the Coma-Sculptor Cloud (cloud number 14), group −10, while NGC 2787 is placed in the Ursa Major Cloud (cloud number 12), group −0. Of the galaxies discussed, only M81 and NGC 3077 are part of the galaxy sample used by Nolthenius 1993 (hereafter N93) for his group compilation. Both galaxies are listed as members of the M81 group (group number 40). The dwarf ellipticals BK5N and F8DI and their membership to the M81 group are discussed by Caldwell et al. (1998) and Karachentseva (1985).

The NGC 5128 Group. The group is quite sparse and extended. NGC 5102 and NGC 5253 are found 7° and 14° north respectively of NGC 5128, the brightest galaxy in the group. Both NGC 5102 and NGC 5128 are isolated, while NGC 5253 is located in a sub-clump of 3 galaxies (one of which is NGC 5236, the brightest spiral in the area), all within 2°×2° and 100 km s^{-1} in redshift. Because NGC 5128, NGC 5102 and NGC 5253 and NGC 5236 have very similar systemic velocity (the total range spanned is 150 km s^{-1} at 500 km s^{-1} redshift), and because of the lack of obvious sub-clumping, physical association has been assumed. All three galaxies listed in the NGC 5128 group are classified as part of the Coma-Sculptor Cloud (cloud number 14), group −15 by T88.

The M101 Group. M101 (NGC 5457) is the brightest member of the group, which is very loose (as for the NGC 5128 group, it is not possible to identify a well defined core: only two galaxies, NGC 5477 and 13529+5409 are found within a 2° radius and 1000 km s^{-1} in systemic velocity). NGC 5195 is found in a small sub-clump of three galaxies about 8° south-east of M101, while NGC 5866 is located in a sub-clump of four galaxies 10° in the opposite direction. Because of the good agreement in systemic velocities, NGC 5195 and NGC 5866 have have been classified as possible members of the M101 group, in spite of the large spatial separation. However, note that both N93 and T88 place the three galaxies in different clouds or groups: N93 classifies NGC 5866 in group No. 147, and NGC 5195 in the M51 group (group number 115, NGC 5102 is not part of the catalog); T88 places NGC 5457 and NGC 5195 in the Coma-Sculptor Cloud, but the first in group −9, and the second in group −5, while NGC 5866 is located in the Draco Cloud (cloud number 44), group −1.

The NGC 1023 Group. The group is very well defined. All of the galaxies classified as certain members are found within 6° of NGC 1023 and have very similar systemic velocity. NGC 855, for which an SBF distance exists, is located 12° away from NGC 1023, and 6° from NGC 925, which is itself at the outer boundary of the core region. The systemic velocity of NGC 855 is only 50 km s^{-1} lower than for NGC 1023. Because no other obvious member of the group is located outside

a 6° radius from NGC 1023, we classify NGC 855 as a probable, rather than certain member. Unfortunately, NGC 855 is not included in either the N93 or the T88 catalogs. T88 classifies all of our certain members of the NGC 1023 group as belonging to the Triangulum spur (cloud number 17), group −1. NGC 891 is further placed in the first level association +1.

The NGC 3184 Group. The core of the group is defined by NGC 3184, NGC 3198 and NGC 3319. These are all located within 3° of each other, and show very good agreement in their systemic velocities. NGC 3413 is located 13° south-west of the core. However, the galaxy has the same systemic velocity as NGC 3198, and one additional galaxy with very similar velocity, NGC 3432, is located 7° SW of the group core, bridging NGC 3413 to the center. For these reasons, and in spite of the large spatial separation, we list NGC 3413 as a probable member of the group. Unfortunately, NGC 3413 is not part of the T88 or N93 catalogs. T88 places both NGC 3198 and NGC 3319 in the Leo Spur (cloud number 15), group +7.

The Leo I Group. All of the galaxies classified as certain members are within 2°×2° and 230 km s^{-1}. About 8° north-east, and at the same systemic velocity as the Leo I group (as defined above) is the very tight quartet formed by NGC 3599, NGC 3605, NGC 3607 and NGC 3608. The SBF distances to these galaxies place the group over one magnitude farther than Leo I, excluding physical associations between the two groups. About 6° east we find a tight quartet formed by the late type spirals NGC 3623, NGC 3627, NGC 3628 and NGC 3593 at the same systemic velocity as, and possibly associated with, the Leo I group. All of the galaxies listed as certain members of the Leo I group are also classified as such in the N93 (group number 50) and T88 (Leo Spur, group +7) catalogs.

The NGC 7331 Group. NGC 7331 and NGC 7457 are about 7° from each other, and have the same heliocentric velocity. T88 assigns the two galaxies to the same cloud but different groups. We classify their physical association as probable.

The Coma I and Coma II Clouds. This is a very complex region, and group association cannot be established with confidence for any of the galaxies. The highest concentration of galaxies appears to be at the location of NGC 4278 and NGC 4283, which have systemic velocities of 643 km s^{-1} and 1076 km s^{-1} respectively. The other six galaxies within 1° of the pair have systemic velocities in between these two extremes. NGC 4414 is standing alone 2° to the north-east, with a systemic velocity of 720 km s^{-1}. Because of its proximity to the core, the lack of association with any other obvious group, and the agreement in systemic velocities, we consider it probably associated with the Coma I cloud. The same is true for NGC 4251 (systemic velocity 1067 km s^{-1}), which is located 2° to the south-west. NGC 4627 is located almost 4° north-east of NGC 4414, in a group of three galaxies with systemic velocity around 700 km s^{-1}. Because of the agreement in systemic velocity we consider NGC 4627 as a likely member of the Coma I cloud. Our analysis largely agrees with N93, who list NGC 4251, NGC 4283, NGC 4414 and NGC 4627 as members of the Coma I cloud (group number 81), but NGC 4278 as part of a sub-clump of five galaxies (group number 100). NGC 4150 is found within 2° of the core, but because of its low systemic

velocity (226 km s^{-1}), we classify it as a probable, rather than a certain member of the cluster. A small sparse group of five galaxies (NGC 4565, NGC 4494, NGC 4562, NGC 4747 and NGC 4725) lies about 6° to the south-east of the core of the Coma I cloud. All of the galaxies in this group, which we identify as the Coma II cloud, have systemic velocities in the narrow range 1190 km s^{-1} to 1395 km s^{-1}, outside the range spanned by the galaxies identified as certain members of the Coma I cloud (600 to 1000 km s^{-1}). The group extends for about 4° in the east-west direction. All of the galaxies which are here classified as part of the Coma I or II clouds are placed in the Coma-Sculptor Cloud, group −1, by T88, with the exception of NGC 4627 (which is not included in the catalog) and NGC 4725, which is placed in group −2, first level association +1.

The Virgo Cluster. The structural complexity of the Virgo cluster has been recognized and studied for more than thirty years (e.g. de Vaucouleurs & de Vaucouleurs, 1973). We limit our analysis to the regions where galaxies with Cepheid distances are found. For these regions, Table 6 summarizes the spatial and kinematical structure identified by different authors within the cluster. In spite of the complication introduced by the fact that a succession of authors have used different criteria and different nomenclature to describe the structure within the cluster, all agree on identifying two prominent sub-structures, defined by the projected density of galaxies. These structures are associated with, but not centered on, the two brightest Virgo galaxies, M87 and NGC 4472. We follow Huchra (1985) and refer to these as the M87 sub-cluster and the NGC 4472 sub-cluster. Table 6 shows that the mean velocities of the two sub-clusters, measured within a 2° radius, are the same. When higher velocity spirals located at larger radii from the center are included, the mean velocity for the NGC 4472 sub-cluster increases while the mean velocity for the M87 sub-cluster remains approximatively constant. The two sub-clusters also differ in their ratio of spirals to ellipticals, which is smaller in the M87 than in the NGC 4472 sub-cluster.

The physical reality of the two sub-clusters is confirmed by X-ray data. The Rosat observations of the Virgo cluster (Böhringer et al. 1994) show in beautiful detail the distribution of X-ray emitting gas first detected by the Einstein and Exosat satellites. These observations show that the Virgo cluster core is filled with hot gas, and that the M87 sub-cluster corresponds to the deepest potential well. In contrast to the fact that neither M87 nor NGC 4472 are at the geometrical center of the galaxies isopleths, to first order each galaxy is at the center of the X-ray emitting corona and, consequently, of the dark mass that dominates the cluster, with M87 having the lion's share. Based on velocities and Tully-Fisher and fundamental plane distances to 59 early-type and 75 late-type galaxies, Gavazzi et al. (1999) conclude that the M87 and NGC 4472 sub-clusters are at the same distance (a conclusion also supported by the SBF observations presented in Ajhar et al. 1999).

Of the galaxies with Cepheid distances, NGC 4321, NGC 4548 and NGC 4571 are located in the the M87 sub-cluster, while NGC 4535 is located in the NGC 4472 sub-cluster. The association of NGC 4536 and NGC 4496A is more problematic, as the galaxies are found over 5° south of NGC 4472. According to Gavazzi et al. (1999) the two galaxies are within the NGC 4472 sub-cluster, which they extend farther south than previous authors, and beyond the region

dominated by the X-ray emission associated with NGC 4472 (even if NGC 4496A is not included in the Gavazzi et al. survey, its location and its systemic velocity place it within the sub-cluster). Therefore we include all three galaxies in the NGC 4472 sub-cluster; in practice this decision is of little consequence as the three galaxies have very similar Cepheid distances.

In addition to the two sub-clusters described above, Gavazzi et al. (1999) identify several other clumps, one of which, named the 'E cloud', is located to the east of the M87 sub-cluster and contains our last Cepheid galaxy, NGC 4639. Cloud E is found to have the same recessional velocity as the M87 sub-cluster, but is $\sim 0.4 \pm 0.2$ mag in the background. In keeping with Huchra's nomenclature, we rename this region as the NGC 4649 (M60) sub-cluster from the most prominent galaxy found here. We would like to stress that while the physical association of galaxies in the M87 and NGC 4472 sub-clumps is well established, this is not the case for the NGC 4649 sub-clump, and in fact SBF distances in this region (Ajhar et al. 1999, Ferrarese et al. 2000a) are very heterogeneous and point to a more complex structure than envisioned by Gavazzi et al. (1999).

We would like to spend a few extra words regarding the confinement of NGC 4639 to a different region of the Virgo cluster than M87 and NGC 4472 which, as described above, are likely to define the cluster's center. The issue is particularly important, because the Cepheid distance modulus to NGC 4639 is ~ 31.9 mag, while the remaining five Cepheid galaxies have distance modulus ~ 31.0 mag, with very small dispersion. The reasonable doubt here is that M100, NGC 4494A, NGC 4535, NGC 4536 and NGC 4548 might be at the near side of the cluster, while NGC 4639 might be at the far side, and therefore the 'true' distance to the Virgo cluster would be better defined by the mean of all six Cepheid distances, rather than by the mean of the five 'nearby' galaxies. In addition to the (admittedly not very strong) evidence reported above that NGC 4639 lies in a clump that seems to be at slightly larger distances than the region around M87 and NGC 4472, there are two strong reasons to reject NGC 4639 in determining the distance to the Virgo cluster. The first is based on simple geometrical arguments: NGC 4639 is located 3° east of M87, which is also the radius of the cluster's core as defined by Huchra (1985). If the cluster is approximatively spherical, then the back to front depth of the core corresponds to 0.2 mag in distance modulus. NGC 4639 is ~ 0.8 mag more distance than the other Cepheid galaxies, implying that it is background to the cluster. The question remains whether the remaining five Cepheid galaxies are indeed representative of the Virgo cluster mean distance. The strongest argument in support of this hypothesis is from Böhringer et al. (1997) and Vollmer et al. (1999) who found that NGC 4548 shows clear signs of its interstellar medium being stripped and distorted as a consequence of the galaxy passing close to the center of the potential well of the cluster.

Galaxies with PNLF, TRGB, GCLF and SBF distances are placed in one of the three sub-clusters in the Virgo cluster (M87, NGC 4472 and NGC 4649); for those galaxies which are not included in the Gavazzi study, the classification was based on redshift and position, and it was unambiguous in all cases.

Figure 2 shows the Rosat X-ray map of the Virgo cluster (from Böhringer et al. 1994). The straight lines define the regions into which Gavazzi et al. (1999) divide the cluster. The circles, triangles and squares show the location of the galaxies with Cepheid, SBF, GCLF and PNLF distances presented in this paper.

The Fornax Cluster. As for the Virgo cluster, we follow previous studies of the Fornax cluster region rather than attempting a new classification. The Fornax cluster is not included in the N93 catalog. We consider as certain members of the cluster all galaxies classified by T88 as belonging to the Fornax cluster + Eridanus Cloud (cloud number 51), group -1. All of these galaxies, with the exception of NGC 1316, are found in the core of the cluster within a $2^\circ \times 2^\circ$ region, and have systemic velocities between 1350 km s^{-1} and 1950 km s^{-1}. To these galaxies, we added NGC 1373, NGC 1380A and NGC 1380B, which are not included in the T88 catalog, but are found in the same confined region of phase space as the rest of the galaxies. NGC 1316 is located $3^\circ\!.5$ SW of the core, and classified as a true cluster member by T88. As a consequence, we also classify NGC 1326A (not part of the T88 catalog) as a true member, because it lies only half a degree away from NGC 1316, and shares the same systemic velocity. All of the galaxies discussed above are also listed as true members of the Fornax cluster by Ferguson (1989). ESO358-G6, ESO358-G59, IC 1919, NGC1336, NGC 1339, NGC 1351 and NGC 1419 are found between 2° and 3° from the core. T88 discusses only NGC 1339, and places it in group +2, first level association +1. However, Ferguson (1989) considers all of the above galaxies as true members, and because we see no reason to isolate NGC 1339 (which has a systemic velocity of ~ 1370 km s^{-1}, very close to the cluster mean), we classify all of the above galaxies as true members. Likewise, IC 2006 and NGC 1366 are not discussed by either T88 or Ferguson (1989), although they are found within 3° of the cluster core and have systemic velocities very typical for the cluster. NGC 1425 and NGC 1344 are 6° and 4.5° north of the core respectively, and therefore not included in the Ferguson study (which is limited to the inner $3^\circ\!.5$ of the cluster). T88 places NGC 1425 in group -0, first level association +1, and NGC 1344 in group +2, first level association +1. Following the discussion in Mould et al. (2000) we list these galaxies as certain members of the Fornax cluster. All of the galaxies mentioned above are within one Abell radius of the cluster center (Giovanelli et al. 1997).

The Eridanus cluster. There are no Cepheid distances to the Eridanus cluster, however, there are both I and K' SBF distance to four of its galaxies. NGC 1395 and NGC 1426 are listed by T88 as belonging to group 51, cloud -4, and are certain members of the cluster. NGC 1407 is also in the core of the cluster, and has a redshift only 60 km s^{-1} higher than NGC 1395. We consider N1407 a true member in spite of it being classified in cloud -8 by T88. NGC 1400 is projected in the cluster core, and it is placed in group +8 by T88. Its velocity is only 550 km s^{-1}, much lower than the cluster mean (~ 1600) km s^{-1}, and we therefore consider it as a possible member.

REFERENCES

Armandroff, T. E., Davies, J. E., & Jacoby, G. H. 1998, AJ, 116, 2287

Ajhar, E. A., Blakeslee, J.P., & Tonry, J.L. 1994, AJ, 108, 2087

Ajhar, E. A., et al. 1997, AJ, 114, 626

Ajhar, E. A., et al. 1999, in preparation

Baum, W., et al. 1995, AJ, 110, 2537

Baum, W., et al. 1996, BAAS, 189, 1204

Baum, W., et al. 1997, AJ, 113, 1483

Bender, R., Burstein, D., & Faber, S. M. 1993, ApJ, 411, 153

Bianchi, L., et al. 1996, ApJ, 471, 203

Binggeli, B., Tammann, G.A., & Sandage, A. 1987, AJ, 94, 251

Blakeslee, J.P., Ajhar, E. A., & Tonry, J.L. 1998 x

Blakeslee, J.P., & Tonry, J.L. 1996, ApJL, 465, L19

Böhringer, H., Neumann, S., Schindler, S., & Huchra, J. P. 1997, ApJ, 485, 439

Böhringer, H., et al. 1994, Nature, 368, 828

Bridges, T.J., Hanes, D.A., & Harris, W.E. 1991, AJ, 101 469

Burstein, D., & Heiles, C. 1984, ApJS, 54, 33

Caldwell, N, Armandroff, T. E., Da Costa G. S., & Seitzer, P. 1998, AJ, 115, 535

Caputo, F., et al. 1999, AJ, 117, 2199

Cardelli, J. A., Clayton, G. C., & Mathis, J. S. 1989, ApJ, 345,245

Ciardullo, R., Jacoby, G.H., Feldmeier, J. J., & Bartlett, R. E. 1998, ApJ, 492, 62

Ciardullo, R., Jacoby, G.H., & Ford, H.C. 1989, ApJ, 344, 715

Ciardullo, R., Jacoby, G.H., Ford, H. C., & Neill, J. D. 1989, ApJ, 339, 53

Ciardullo, R., Jacoby, G.H., & Harris, W.E. 1991, ApJ, 383, 487

Ciardullo, R., Jacoby, G.H., & Tonry, J.L. 1993, ApJ, 419, 479

De Vaucouleurs, G., & De Vaucouleurs, A. 1973, A&A, 28, 109

de Vaucouleurs, G., de Vaucouleurs, A., Corwin, H. G., Buta, R. J., Paturel, G., & Fouque, P. 1991, Third Reference Catalog of Bright Galaxies, New York: Springer

Della Valle, M., Kissler-Patig, M., Danziger, J., & Storm, J. 1998, MNRAS, 299 267

Durrell, P., McLaughlin, D., Harris, W., & Haynes, D. 1996, ApJ, 463, 543

Elson, R. A. W. 1997, MNRAS, 286, 77

Elson, R. A. W., & Santiago, B. X. 1996, MNRAS, 280, 971

Elson, R. A. W., et al. 1998, MNRAS, 295, 240

Faber, S. M., Wegner, G., Burstein, D., Davies, R. L., Dressler, A., Lynden-Bell, D., & Terlevich, R. J. 1989, ApJS, 69, 763

Feldmeier, J., Ciardullo, R., & Jacoby, G.H. 1996, ApJL, 461, 25

Feldmeier, J., Ciardullo, R., & Jacoby, G.H. 1997, ApJ, 479, 231

Ferguson, H. C. 1989, AJ, 98, 367

Ferguson, H. C., Tanvir, N. R., & von Hippel, T. 1998, Nature, 391, 461

Ferrarese, L., et al. 1996, ApJ, 464, 568

Ferrarese, L., et al. 1998, ApJ, 507, 655

Ferrarese, L., et al. 2000a, ApJ, in press (astro-ph/9908192)

Ferrarese, L., et al. 2000b, PASP, submitted

Ferrarese, L., et al. 1999, in the Proceedings of the Cosmic Flows Workshop, Victoria, Canada, July 1999, eds. S. Courteau, M. Strauss & J. Willick, ASP series. (astro-ph/9909134)

Ferraro, F. R., Fusi Pecci, F., Tosi, M., & Buonanno, R. 1989, MNRAS, 241, 433

Fischer, P., Hesser, J. E., Harris, H. C., & Bothun, G. D. 1990, PASP, 102, 5

Fleming, D., Harris, W., Prichet, C., & Hanes, D. 1995, AJ, 109, 1044

Forbes, D. 1996a, AJ, 112, 1409

Forbes, D. 1996b, AJ, 112, 954

Forbes, D., Brodie, J., & Grillmair, C. J. 1997, AJ, 113, 1652

Ford, H.C., et al. 1996, ApJ, 458, 455

Freedman, W. L. 1988, ApJ, 326, 691

Freedman, W. L. 1988, AJ, 96, 1248

Freedman, W. L., & Madore, B. F. 1988, ApJL, 332, L63

Freedman, W. L., Wilson, C. D., Madore, B. F. 1991, ApJ, 372, 455

Freedman, W. L. et al. 1992, ApJ, 396, 80

Freedman, W. L. et al. 1994, ApJ 427, 628

Gallart, C., Aparicio, A., & Vilchez, J. M. 1996, AJ, 112, 1928

Gavazzi, G., et al. 1999, MNRAS, 304, 595

Geisler, D. 1996, AJ, 111, 480

Gibson, B., et al. 1999, ApJ, 512, 48

Gibson, B., et al. 2000, in press (astro-ph/9908149)

Giovanelli, R., et al. 1997, AJ, 113, 22

Golev, V., Prugniel, P. H., Simien, F., Longhetti, M. 1999, A&AS, 136, 519

Gorgas, J., Efstathiou, G., & Salamanca, A. A. 1990, MNRAS, 245, 217

Graham, J. A., et al. 1997, ApJ, 477, 535

Graham, J. A., et al. 1998, ApJ, 512, 48

Grebel, E., & Guhathakurta, P. 1999, ApJL, 511, 101

Grillmair, C. J., Forbes, D. A., Brodie, J., & Elson, R. 1999, AJ, 117, 167

Harris, W. 1990, PASP, 102, 966

Harris, W., Allwright, J., Pritchet, C., & van den Bergh, S. 1991, ApJS, 76, 115

Harris, W. E., Durrell, P. R., Pierce, M. J., & Secker, J. 1998, Nature, 395, 48

Hill, R. J. et al. 1998, ApJ, 496, 648

Hoessel, J. G., Saha, A., & Danielson, G. E. 1998, AJ, 115, 583

Holtzman, J. A. et al. 1995, PASP, 107, 1065

Hopp, U., Schulte-Ladbeck, R. E., Greggio, L., & Mehlert, D. 1999, A&A, 342, L9

Huchra, J. P. 1985 in 'ESO Workshop on the Virgo Cluster of Galaxies', Garching, West Germany, European Southern Observatory, eds. O.-G. Richter and B. Binggeli, p. 181

Huchra, J., & Mader, J. 1998, http://cfa-www.harvard.edu/∼huchra, ZCAT Version July 15, 1998

Huchra, J. P., et al. 1996, ApJS, 102, 29

Hughes, S.,M. et al. 1998, ApJ, 501, 32

Hui, X., et al. 1993, ApJ, 414, 463

Humphreys, R. M., et al. 1986, AJ, 91, 808

Jacoby, G. H. 1996, The Extragalactic Distance Scale, Proceedings of the ST ScI May Symposium, Eds.: M. Livio, M. Donahue, and N. Panagia, Cambridge University Press, p. 197

Jacoby, G.H., Ciardullo, R., Booth, J., & Ford, H. C. 1989, ApJ, 344, 70

Jacoby, G.H., Ciardullo, R., & Ford, H.C. 1990, ApJ, 356, 332

Jacoby, G.H., Ciardullo, R., & Harris, W.E. 1996, ApJ, 462, 1

Jacoby, G.H., Walker, A.R., & Ciardullo, R. 1990, ApJ, 365, 461

Jacoby, G. H., et al. 1992, PASP, 104, 599

Jensen, J. B., Tonry, J. L., & Luppino, G. A. 1998, ApJ, 505, 111

Jensen, J. B., et al. 1998, BAAS, 192, 5202

Karachentseva, V. E., Karachentsev, I. D., & Börngen, F. 1985, A&AS, 60, 213

Kaufman, M., Bash, F. N., Kennicutt, R.C., & Hodge, P. W. 1987, ApJ, 319, 61

Kelson, D., et al. 1996, ApJ, 463, 26

Kelson, D., et al. 1999, ApJ, 514, 614

Kelson, D., et al. 2000, ApJ, in press (astro-ph/9909222)

Kennicutt, R. C. 1999, in preparation

Kennicutt, R. C., Freedman, W. L., & Mould, J. R. 1995, AJ, 110, 1476

Kennicutt, R. C., et al. 1998, ApJ, 498, 181

Kissler, M. et al. 1994, A&A, 287, 463

Kissler-Patig, M., Richtler, T., Hilker, M. 1996, A&A, 308, 704

Kohle, S., Kissler-Pattig, M., Hilker, M., Richtler, T., Infante, L., & Quintana, H. 1996, A&A, 309, L39

Kundu, A., & Whitmore, B. C. 1998, AJ, 116, 2841

Kundu, A., et al. 1999, ApJ, 513, 983

Lauer, T. R., Tonry, J. L., Postman, M., Ajhar, E. A., & Holtzman, J. A. 1998, ApJ, 499, 577

Lee, M. G. 1993, ApJ, 408, 409

Lee, M. G. 1995a, AJ, 110, 1129

Lee, M. G. 1995b, AJ, 110, 1155

Lee, M. G., & Byun, Y.-I. 1999, astro-ph/9905061

Lee, M. G., Freedman, W.L., & Madore, B.F. 1993, ApJ, 417, 552

Lee, M. G., Freedman, W. L., & Madore, B. F. 1993, in 'New Perspectives on Stellar Pulsations and Pulsating Variable Stars', IAU Colloq. 139, eds. J. Nemec and J. Matthews

Lee, M.G., Kim, E., & Geisler, D. 1998, AJ, 115, 947

Lequeux, J., et al. 1979, A&A, 80, 155

Macri, L., et al. 1999, astro-ph/9901332

Masegosa, J., Moles, M., Campos-Aguilar, A. 1994, A&A, 249, 505

Madjesky, R., & Rabolli, M. 1995, A&A, 297, 660

Madore, B. F., & Freedman, W. L. 1991, PASP, 103, 933

Madore, B. F., Freedman, W. L., & Sakai, S. 1996, The Extragalactic Distance Scale, Proceedings of the ST ScI May Symposium, Eds.: M. Livio, M. Donahue, and N. Panagia, Cambridge University Press, p. 239

Massey, P., & Armandroff, T. E. 1995, AJ, 109, 2470

McMillan, R., Ciardullo, R., & Jacoby, G.H. 1993, ApJ, 416, 62

McMillan, R., Ciardullo, R., & Jacoby, G.H. 1994, AJ, 108, 1610

Minniti, D., Zijlstra, A. A., & Victoria Alonso, M. 1999, AJ, 117, 881

Mould, J. R., & Kristian, J. 1986, ApJ, 305, 591

Mould, J. R., Kristian, J., & Da Costa, G. S. 1984, ApJ, 278, 575

Mould, J.R., et al. 1999, ApJ, in press

Mould, J.R., et al. 2000, ApJ, in press (astro-ph/9909260)

Musella, I., Piotto, G., & Capaccioli, M. 1997, AJ, 114, 976

Neilsen, E. H., Tsvetanov, Z., & Ford, H.C. 1997, ApJ, 483, 745

Neilsen, E. H., Tsvetanov, Z., & Ford, H.C. 1997, astro-ph/9712339

Nolthenius, R. 1993, ApJS 85, 1

Oey, M. S., & Kennicutt, R. C. 1993 ApJ, 411, 1370

Ostrov Forte Geisler 1998

Pagel, B. E. J., Edmunds, M. G., Fosbury, R. A. E., & Webster, B. L. 1978, MNRAS, 184, 569

Pagel, B. E. J., Edmunds, M. G., & Smith, G. 1980, MNRAS, 193, 219;

Pahre, M. A., & Mould, J. R. 1994, ApJ, 433, 567

Pahre, M. A., et al. 1999, ApJ, 515, 79

Perelmuter, J.M., & Racine, R. 1995, AJ, 109, 1055

Perrett, K.M., Hanes, D.A., Butterworth, S.T., & Kavelaars, J.J. 1997, AJ, 113, 895

Phelps R. et al. 1998, ApJ, 500, 763

Phillips, M. M., et al. 1992, BAAS, 180, 1304

Pierce, M. J., et al. 1994, Nature, 371, 385

Pritchet, C., & van den Bergh, S. 1985, AJ, 90, 2027

Prosser, C. F., et al. 1999 astro-ph/9906486

Rawson, D.,M. et al. 1997, ApJ, 490, 517

Reed, L. G., Harris. G. L. H., & Harris, W. E. 1994, AJ, 107, 555

Reid, N., Mould, J. R., & Thompson, I. 1987, ApJ, 323. 433

Richer, M. G., & McCall, M.L. 1992, AJ, 103, 54

Richtler, T., et al. 1992, A&A, 264, 25

Saha, A., Labhardt, L., Schwengeler, H., Macchetto, F. D., Panagia, N., Sandage, A., & Tammann, G. A. 1994, ApJ, 425, 14

Saha, A., Sandage, A., Labhardt, L., Schwengeler, H., Tammann, G. A., Panagia, N., & Macchetto, F. D. 1995, ApJ, 438, 8

Saha, A., Sandage, A., Labhardt, L., Tammann, G. A., Panagia, N., & Macchetto, F. D. 1996a, ApJ, 466, 55

Saha, A., Sandage, A., Labhardt, L., Tammann, G. A., Panagia, N., & Macchetto, F. D. 1996b, ApJS, 107, 693

Saha, A., Sandage, A., Labhardt, L., Tammann, G. A., Macchetto, F. D., & Panagia, N. 1997, ApJ, 486, 1

Saha, A., Sandage, A., Tammann, G. A., Labhardt, L., Macchetto, F. D., & Panagia, N. 1999, astro-ph/9904389

Sakai, S. 1999, in 'Cosmological Parameters and the Evolution of the Universe', IAU Symposium no. 183, Kyoto, Japan, ed. K. Sato, Dordrecht, Boston : Kluwer Academic, p. 48

Sakai, S., & Madore, B. F. 1999, astro-ph/9906484

Sakai, S., Madore, B.F., & Freedman, W.L. 1996, ApJ, 461, 713

Sakai, S., Madore, B. F., & Freedman, W. L. 1997, ApJ, 480, 589

Sakai, S., Madore, B.F., & Freedman, W.L. 1999, ApJ, 511, 671

Sakai, S., et al. 1997, ApJ, 478, 49

Sakai, S., et al. 1999, ApJ, in press (astro-ph/9906487)

Sakai, S., et al. 2000, ApJ, in press (astro-ph/9909269)

Sandage, A. 1988, PASP, 100, 935

Sandage, A., & Carlson, G. 1985, AJ, 90, 1464

Schlegel, D. J., Finkbeiner, D. P., & Davis, M. 1998, ApJ, 500, 525

Silbermann, N. A. et al. 1996, ApJ, 470, 1

Silbermann, N. A. et al. 1999, ApJ, 515, 1

Skillman, E. D., Kennicutt, R. C., & Hodge, P. W. 1989, ApJ, 347, 875

Skillman, E. D., Melnick, J., Terlevich, R., Moles, M. 1988, A&A, 196, 31

Soffner, T., et al. 1996, A&A, 306, 9

Soria, R., et al. 1996, ApJ, 465, 79

Stetson, P. B., et al. 1998, ApJ, 508, 491

Tanaka, K. I. 1985, PASJ, 37, 133

Thomsen, B., Baum. W.A., Hammergren, M., & Worthey, G. 1997, ApJ, 483, L37

Tolstoy, E., Saha, A., Hoessel, J. G., & Danielson, G. E. 1995a, AJ, 109, 579

Tolstoy, E., Saha, A., Hoessel, J. G., & McQuade, K. 1995b, AJ, 110, 1640

Tolstoy, E., et al. 1998, AJ, 116, 1244

Tonry, J. L. 1996, The Extragalactic Distance Scale, Proceedings of the ST ScI May Symposium, Eds.: M. Livio, M. Donahue, and N. Panagia, Cambridge University Press, p. 297

Tonry, J.L, Blakeslee, J.P., Ajhar, E.A., & Dressler, A. 1997, ApJ, 475, 399

Saha, A., Sandage, A., Labhardt, L., Tammann, G. A., Macchetto, F. D., & Panagia, N. 1997, ApJ, 486, 1

Tully, R. B. 1988, 'Nearby Galaxies Catalog', Cambridge and New York, Cambridge University Press.

Turner, A. et al. 1998, ApJ, 505, 207

Vollmer, B., et al. 1999, astro-ph/9907351

Webster Smith 1983

Welch, D. L., McAlary, C. W., Madore, B. F., McLaren, R. A., & Neugembauer, G. 1985, ApJ, 292, 217

Welch, D. L., McLaren, R. A., Madore, B. F., & McAlary, C. W. 1987, ApJ, 321, 162

Whitmore, B. 1996, The Extragalactic Distance Scale, Proceedings of the ST ScI May Symposium, Eds.: M. Livio, M. Donahue, and N. Panagia, Cambridge University Press, p. 254

Zaritsky, D., Kennicutt, R. C., & Huchra, J. P. 1994, ApJ, 420, 87

Fig. 1a.— Finding charts showing all galaxies identified by zcat (Huchra & Mader 1998) in the vicinity of each group considered in this paper, within the velocity range shown in each panel. The coordinates are at J2000; the galaxy heliocentric velocity is defined by the color code as shown in the bar on top of each panel, while the symbol size is proportional to the galaxy B magnitude reported in Table 1. Galaxies for which a Cepheid distance exists are shown as filled pentagons; galaxies with SBF, PNLF, TRGB and GCLF distances are shown as open circles, squares, hexagons and triangles respectively. All other galaxies are shown as open stars.

Fig. 1b.— As for Figure 1a.

Fig. 2.— The Rosat X-ray map of the Virgo cluster (from Böhringer et al. 1994). The straight lines define the regions into which Gavazzi et al. (1999) divide the cluster. The circles, triangles and squares show the location of the galaxies with Cepheid, SBF, GCLF and PNLF distances presented in this paper.

Table 1. Galaxy Properties

Name(s)	RA (J2000)[a]	DEC (J2000)[a]	Type[b]	T[a]	B_T[a]	$v\pm\delta\ v$ [b]
WLM	00h01m57s	−15°27′01″	IB(s)m	10.0±0.3	11.03±0.08	−116±2
IC10	00 20 25	+59 17 30	IBm?	10.0±0.3	11.81±0.12	−344±3
N205 M110	00 40 22	+41 41 11	E5 pec	−5.0±0.3	8.92±0.05	−241±3
N221 M32	00 42 42	+40 51 55	cE2	−6.0±0.3	9.03±0.05	−205±8
N224 M31	00 42 44	+41 16 08	SA(s)b	3.0±0.3	4.36±0.02	−300±4
SMC	00 52 38	−72 48 01	SB(s)m pec	9.0±0.3	2.70±0.10	158±4
N300	00 54 54	−37 40 57	SA(s)d	7.0±0.3	8.72±0.05	144±1
LGS3	01 03 48	+21 53	I?	···	···	−277±5
IC1613	01 04 48	+02 07 10	IB(s)m	10.0±0.3	9.88±0.09	−234±1
And V dSph[c]	01 10 17	+47 37 41	dSph	···	···	···
N598 M33	01 33 51	+30 39 37	SA(s)cd	6.0±0.3	6.27±0.03	−179±3
N708	01 52 46	+36 09 06	E	−5.0±0.7	13.70±0.30	4813±24
N720	01 53 00	−13 44 17	E5	−5.0±0.3	11.16±0.05	1716±11
N855	02 14 04	+27 52 38	E	−5.0±0.7	13.30±0.13	610±10
N891	02 22 33	+42 20 48	SA(s)b? sp	3.0±0.3	10.81±0.18	528±4
N925	02 27 17	+33 34 41	SAB(s)d	7.0±0.3	10.69±0.11	553±3
N949	02 30 49	+37 08 09	SA(rs)b:?	3.0±0.7	12.40±0.14	609±2
N1023	02 40 24	+39 03 46	SB(rs)0−	−3.0±0.3	10.35±0.06	637±4
N1316	03 22 42	−37 12 28	(R')SAB(s)0^0	−2.0±0.3	9.42±0.08	1793±12
N1326A	03 25 09	−36 21 54	SB(s)m:	8.8±0.4	13.77±0.21	1836±8
IC1919	03 26 02	−35 53 45	SA(rs)0−?	−3.0±0.4	13.80±0.10	1220±29
N1336	03 26 31	−35 42 52	SA0−	−3.3±0.4	13.10±0.09	1421±9
E358−G006	03 27 18	−34 31 37	S0(9)	−3.7±0.7	13.92±0.14	1237±32
N1339	03 28 06	−32 17 10	E4	−4.4±0.3	12.51±0.13	1367±9
N1344	03 28 19	−31 04 05	E5	−5.0±0.3	11.27±0.10	1169±15
N1351	03 30 35	−34 51 12	SA0− pec:	−3.0±0.4	12.46±0.13	1511±9
N1365	03 33 37	−36 08 17	(R')SBb(s)b	3.0±0.3	10.32±0.07	1636±1
N1366	03 33 53	−31 11 36	$S0^0$	−2.0±0.6	11.97±0.13	1297±25
N1373	03 34 59	−35 10 16	E+:	−4.3±0.6	14.12±0.08	1385±18
N1375	03 35 17	−35 15 59	$SAB0^0$: sp	−2.0±0.5	13.18±0.13	740±6
N1379	03 36 03	−35 26 26	E3	−5.0±0.4	11.80±0.10	1380±12
N1374	03 36 17	−35 13 35	E3	−4.5±0.4	12.00±0.08	1352±11
N1380	03 36 27	−34 58 33	SA0	−2.0±0.6	10.87±0.10	1877±12
N1381	03 36 31	−35 17 39	SA0: sp	−1.6±0.5	12.44±0.10	1724±9
N1386	03 36 46	−35 59 58	SB(s)0+	−0.6±0.5	12.09±0.10	868±5
N1380A	03 36 47	−34 44 22	$S0^0$: sp	−2.0±0.8	13.31±0.13	1561±6

Table 1—Continued

Name(s)	RA (J2000)[a]	DEC (J2000)[a]	Type[b]	T[a]	B_T[a]	$v\pm\delta\ v$ [b]
N1387	03 36 57	−35 40 23	SAB(s)0−	−3.0±0.3	11.68±0.10	1302±12
N1380B	03 37 08	−35 11 41	SAB(s)0−:	−2.7±0.6	12.92±0.13	1802±25
N1389	03 37 12	−35 44 42	SAB(s)0−:	−3.3±0.4	12.42±0.13	995±22
N1399	03 38 29	−35 26 58	E1 pec	−5.0±0.3	10.55±0.10	1447±12
N1395	03 38 30	−23 01 40	E2	−5.0±0.3	10.55±0.06	1699±19
N1404	03 38 52	−33 35 36	E1	−5.0±0.3	10.97±0.13	1942±12
N1400	03 39 31	−18 41 19	SA0−	−3.0±0.3	11.92±0.13	558±14
N1407	03 40 12	−18 34 52	E0	−5.0±0.3	10.70±0.20	1779±9
N1419	03 40 43	−37 30 42	E	−5.4±0.5	13.48±0.08	1560±9
N1425	03 42 11	−29 53 40	SAB(rs)b	3.0±0.3	11.29±0.11	1512±3
N1427	03 42 20	−35 23 36	E5	−4.1±0.4	11.77±0.10	1416±6
N1426	03 42 49	−22 06 38	E4	−5.0±0.3	12.29±0.05	1443±6
E358−G059	03 45 03	−35 58 22	SAB0−	−3.0±0.8	13.99±0.13	1007±18
IC2006	03 54 28	−35 58 02	E	−4.5±0.3	12.21±0.10	1364±12
LMC	05 23 35	−69 45 22	SB(s)m	9.0±0.3	0.91±0.05	278±2
N2090	05 47 02	−34 15 05	SA:(rs)b	5.0±0.3	11.99±0.13	931±6
N2403	07 26 54	+65 35 58	SAB(s)cd	6.0±0.3	8.93±0.07	131±3
N2366	07 28 54	+69 12 52	IB(s)m	10.0±0.3	11.53±0.06	100±3
N2541	08 14 40	+49 03 44	SA(s)cd	6.0±0.3	12.26±0.14	559±1
U4305	08 19 06	+70 42 51	Im	10.0±0.3	11.10±0.15	157±1
N2787	09 19 20	+69 12 11	SB(r)0+	−1.0±0.3	11.82±0.14	696±8
F8DI	09 44 47	+67 26 19	dE	···	14.63±0.25	···
N3031 M81	09 55 33	+69 04 00	SA(s)ab	2.0±0.3	7.89±0.03	−34±4
N3034 M82	09 55 54	+69 40 57	I0	···	9.30±0.09	203±4
Leo A	09 59 24	+30 44 42	IBm	−5.0±0.3	12.92±0.18	20±4
Sextans B	10 00 00	+05 19 57	ImIV−V	10.0±0.5	11.85±0.14	301±4
N3109	10 03 07	−26 09 32	SB(s)m	9.0±0.3	10.39±0.07	403±1
N3077	10 03 21	+68 44 02	I0 pec	···	10.61±0.13	14±4
BK5N	10 04 41	+68 15 22	dE	···	17.43±0.25	···
N3115	10 05 14	−07 43 07	S0−	−3.0±1.6	9.87±0.04	663±6
N3115DW1	10 05 41	−07 58 52	SA(s)0^0 pec	···	···	715±62
Leo I	10 08 17	−12 18 27	E	−5.0±0.3	11.18±0.15	168±60
Sextans A	10 11 01	−04 42 48	IBm	10.0±0.3	11.86±0.07	324±1
N3198	10 19 55	+45 33 09	SB(rs)c	5.0±0.3	10.87±0.10	663±4
N3319	10 39 10	+41 41 18	SB(rs)cd	6.0±0.3	11.48±0.17	739±1
N3351 M95	10 43 58	+11 42 15	SB(r)b	3.0±0.3	10.53±0.10	778±4

Table 1—Continued

Name(s)	RA (J2000)[a]	DEC (J2000)[a]	Type[b]	T[a]	B_T[a]	$v\pm\delta\ v$ [b]
N3368 M96	10 46 45	+11 49 16	SAB(rs)ab	2.0±0.3	10.11±0.13	897±4
N3377	10 47 42	+13 59 00	E5−6	−5.0±0.3	11.24±0.10	692±13
N3379 M105	10 47 50	+12 34 57	E1	−5.0±0.3	10.24±0.03	920±10
N3384	10 48 17	+12 37 49	SB(s)0−:	−3.0±0.3	10.85±0.05	735±26
N3412	10 50 53	+13 24 46	SB(s)0^0	−2.0±0.3	11.45±0.13	865±27
N3413	10 51 21	+32 46 04	S0	−2.0±0.4	13.08±0.16	645±6
N3489	11 00 18	+13 54 08	SAB(rs)0+	−1.0±0.3	11.12±0.13	708±10
Leo B	11 13 29	+22 09 12	E0 pec	−5.0±0.3	12.6±0.30	90±60
N3621	11 18 17	−32 48 49	SA(s)d	7.0±0.3	10.28±0.10	727±5
N3627 M66	11 20 15	+12 59 29	SAB(s)b	3.0±0.3	9.65±0.13	727±3
N4150	12 10 33	+30 24 06	SA(r)0^0?	−2.0±0.4	12.44±0.13	226±22
N4251	12 18 08	+28 10 32	SB0? sp	−2.0±0.3	11.58±0.11	1123±29
N4278	12 20 07	+29 16 47	E1−2	−5.0±0.3	11.09±0.13	649±5
N4283	12 20 21	+29 18 40	E0	−5.0±0.4	12.95±0.13	1058±12
N4321 M100	12 22 55	+15 49 23	SAB(s)bc	4.0±0.3	10.05±0.08	1571±1
N4339	12 23 34	+06 04 55	E0	−5.0±0.3	12.26±0.11	1289±9
N4365	12 24 28	+07 19 06	E3	−5.0±0.3	10.52±0.06	1240±12
N4374 M84	12 25 04	+12 53 15	E1	−5.0±0.3	10.09±0.05	1000±8
N4379	12 25 15	+15 36 27	S0− pec:	−2.5±0.5	12.63±0.06	1069±10
N4373	12 25 19	−39 45 37	SAB(rs)0−:	−2.9±0.4	11.90±0.13	3396±18
N4382 M85	12 25 25	+18 11 27	SA(s)0+ pec	−1.0±0.3	10.00±0.07	760±12
N4387	12 25 42	+12 48 42	E5	−5.0±0.6	13.01±0.05	561±15
N4406 M86	12 26 12	+12 56 49	S0(3)/E3	−5.0±0.3	9.83±0.05	−227±8
N4414	12 26 27	+31 13 29	SA(rs)c?	5.0±0.3	10.96±0.13	716±6
N4419	12 27 00	+15 02 52	SA(bs)a	1.0±0.4	12.08±0.10	−261±5
N4434	12 27 37	+08 09 18	E0/S0(0)	−5.0±0.8	13.03±0.06	1071±10
IC3388	12 28 28	+12 49 19	E?	···	15.36±0.07	1704±31
N4458	12 28 58	+13 14 35	E0−1	−5.0±0.4	12.93±0.04	668±15
N4459	12 29 00	+13 58 46	SA(r)0+	−1.0±0.3	11.32±0.04	1210±16
N4468	12 29 31	+14 02 59	SA0−?	−2.6±0.7	13.58±0.07	909±11
N4472 M49	12 29 46	+07 59 58	E2/S0(2)	−5.0±0.3	9.37±0.06	868±8
N4473	12 29 49	+13 25 49	E5	−5.0±0.3	11.16±0.04	2240±9
N4476	12 29 59	+12 20 53	SA(r)0−:	−3.0±0.4	13.01±0.03	1978±12
N4478	12 30 17	+12 19 44	E2	−5.0±0.4	12.36±0.03	1381±13
N4486 M87	12 30 50	+12 23 24	E+0−1 pec	−4.0±0.3	9.59±0.04	1282±9
N4489	12 30 52	+16 45 31	E	−5.0±0.7	12.84±0.11	971±10

Table 1—Continued

Name(s)	RA (J2000)[a]	DEC (J2000)[a]	Type[b]	T[a]	B_T[a]	$v\pm\delta\ v$ [b]
N4494	12 31 24	+25 46 25	E1−2	−5.0±0.3	10.71±0.13	1324±20
N4496A	12 31 39	+03 56 23	SB(rs)m	9.0±0.3	11.94±0.13	1730±3
IG Stars[d]	12 33 52	+12 21 40	N/A	N/A	N/A	N/A
N4526	12 34 03	+07 42 01	SAB(s)0^0	−2.0±0.3	10.66±0.06	448±8
N4531	12 34 16	+13 04 35	SB0+:	−0.5±0.5	12.42±0.15	195±13
N4535	12 34 20	+08 11 53	SAB(s)c	5.0±0.3	10.59±0.08	1961±3
N4536	12 34 27	+02 11 19	SAB(rs)bc	4.0±0.3	11.16±0.08	1804±3
N4548 M91	12 35 26	+14 29 49	SBb(rs)	3.0±0.3	10.96±0.07	486±4
N4550	12 35 31	+12 13 17	$SB0^0$: sp	−1.5±0.5	12.56±0.05	381±9
N4551	12 35 38	+12 15 56	E:	−5.0±0.6	12.97±0.05	1470±10
N4552 M89	12 35 40	+12 33 25	E	−5.0±0.3	10.73±0.05	321±12
N4565	12 36 21	+25 59 05	SA(s)b? sp	3.0±0.3	10.42±0.07	1282±1
N4564	12 36 27	+11 26 21	E6	−5.0±0.5	12.05±0.05	1111±18
N4571	12 36 57	+14 13 03	SA(r)d	6.5±0.5	11.82±0.06	342±3
N4578	12 37 31	+09 33 19	SA(r)0^0:	−2.0±0.5	12.38±0.06	2284±14
N4594 M104	12 39 59	−11 37 22	SA(s)a	1.0±0.3	8.98±0.06	1091±5
N4603	12 40 56	−40 58 33	SA(rs)bc	5.0±0.7	12.29±0.16	2562±8
N4620	12 42 00	+12 56 35	S0	−2.0±0.8	13.2±0.2	1066±50
N4627	12 42 00	+32 34 29	E4 pec	−5.0±0.3	13.06±0.13	765±29
N4621 M59	12 42 02	+12 38 49	E5	−5.0±0.3	10.57±0.06	424±12
N4638	12 42 48	+11 26 35	S0−	−3.0±0.3	12.13±0.04	1164±10
N4636	12 42 50	+02 41 17	$E/S0_1$	−5.0±0.3	10.43±0.10	1095±12
N4639	12 42 53	+13 15 30	SAB(rs)bc	4.0±0.5	12.24±0.10	1010±6
N4649 M60	12 43 40	+11 32 58	E2	−5.0±0.3	9.81±0.05	1413±10
N4660	12 44 32	+11 11 27	E:	−5.0±0.5	12.16±0.04	1097±13
N4725	12 50 27	+25 30 01	SAB(r)ab pec	2.0±0.3	10.11±0.13	1206±3
N4733	12 51 07	+10 54 45	E+:	−4.0±0.5	12.70±0.13	908±23
N4754	12 52 18	+11 18 49	SB(r)0−:	−3.0±0.3	11.52±0.08	1377±15
GR8	12 58 41	+14 13	ImV	10.0±0.9	14.68±0.06	214±3
N4881	12 59 58	+28 14 43	E	−4.0±0.6	14.59±0.08	6705±27
IC4051	13 00 54	+28 00 25	E2	−5.0±0.4	14.17±0.10	4932±22
IC4182	13 05 49	+37 36 21	SA(s)m	9.0±0.4	11.77±0.05	321±1
N5102	13 21 58	−36 37 47	SA0−	−3.0±0.3	10.35±0.10	467±7
N5128 CenA	13 25 29	−43 01 00	S0 pec	−2.0±0.3	7.84±0.06	547±5
N5170	13 29 49	−17 57 59	SA(s)c: sp	5.0±0.5	12.06±0.15	1503±5
N5194 M51a	13 29 53	+47 11 48	SA(s)bc pec	4.0±0.3	8.96±0.06	463±3

Table 1—Continued

Name(s)	RA (J2000)[a]	DEC (J2000)[a]	Type[b]	T[a]	B_T[a]	$v\pm\delta\ v$ [b]
N5195 M51b	13 29 59	+47 16 21	$SB0_1$ pec	···	10.45±0.07	465±10
N5193	13 31 54	−33 14 07	E pec:	−4.5±0.4	12.48±0.14	3723±21
IC4296	13 36 39	−33 57 59	E	−5.0±0.4	11.61±0.05	3761±28
N5253	13 39 56	−31 38 41	Im pec	10.0±0.7	10.87±0.12	404±4
N5457 M101	14 03 12	+54 20 55	SAB(rs)cd	6.0±0.3	8.31±0.09	241±2
N5481	14 06 42	+50 43 34	E+	−4.0±0.6	13.25±0.15	2064±33
N5846	15 06 29	+01 36 25	E0−1	−5.0±0.3	11.05±0.13	1822±9
N5866 M102	15 06 30	+55 45 46	$S0_3$	−1.0±0.3	10.74±0.07	672±9
N6822	19 44 58	−14 48 11	IB(s)m	10.0±0.5	9.31±0.06	−57±2
N7014	21 07 53	−7 10 40	E	−3.8±0.5	13.38±0.13	4764±15
N7331	22 37 05	+34 25 08	SA(s)b	3.0±0.3	10.35±0.10	816±1
N7457	23 01 00	+30 08 39	SA(rs)0−?	−3.0±0.3	12.09±0.11	812±6
UKS2323−326	23 26 28	−32 23 18	IB(s)m pec:	10.0±0.4	13.9±0.2	62±5
Cassiopeia dSph[c]	23 26 31	+50 41 31	dSph	···	16.0±0.5	···
And VI Pegasus dSph[c]	23 51 39	+24 35 42	dSph	···	14.5±0.5	···

[a]Data obtained using the NASA/IPAC Extragalactic Database (NED), version 2.5 (May 27, 1998), except for the M81 group dwarfs BK5N and F8DI, for which data from Caldwell et al. (1998) were used.

[b]Data obtained from the 3rd Reference Catalogue of Bright Galaxies (RC3, de Vaucouleurs et al. 1991), except for the M81 group dwarfs BK5N and F8DI, for which data from Caldwell et al. (1998) were used.

[c]Data from Grebel & Guhathakurta 1999.

[d]This entry refers to the population of intergalactic stars detected by Ferguson et al. (1998) in the Virgo cluster.

TABLES 2 AND 3 ARE IN SEPARATE FILES, AND NEED TO BE INSERTED HERE

Table 4. Revised Cepheid Distances

	Originally Published Distance[a]				Distance from This Paper [b]		
Galaxy	$(m-M)\pm\sigma$	P_{min}	No.	Reference	$(m-M)\pm\sigma$	P_{min}	No.
N1326A	31.36±0.17±0.13	11.4	17	Prosser et al. 1999	31.43±0.07±0.16	20	8
N1365	31.31±0.20±0.18	16.3	34	Silbermann et al. 1999	31.39±0.10±0.16	25	26
N1425	31.73±0.16±0.17	13.3	29	Mould et al. 1999	31.81±0.06±0.16	20	20
N4725	30.50±0.16±0.17	14.0	20	Gibson et al. 1999	30.57±0.08±0.16	20	13
N4535	31.01±0.05±0.26	13.6	39	Macri et al. 1999	31.10±0.07±0.16	25	25

[a]Distance moduli (in mag) originally published in the reference given in column 5. The errors refer to the random and systematic contribution respectively; notice that the uncertainty due to a possible metallicity dependence of the Cepheid PL relation is not considered in this paper. The shorter of the periods used (in days), and the total number of Cepheids used in fitting the PL relation are given in column 3 and 4 respectively.

[a]Distance moduli (in mag) derived by imposing a period cut on the originally published Cepheid sample. The number of Cepheids in the original sample with period larger than the cutoff, and the cutoff period (in days), are listed in columns 8 and 7 respectively.

Table 5. Summary of Groups/Clusters Properties

Group	RA (J2000)[a]	DEC (J2000)[a]	Diameter[b]	No.[c]	v_{hel}[d]	σv[d]
N1023 Group	02h40m	+39°03'	9°	14	601^{+29}_{-17}	83^{+70}_{-30}
Fornax Cluster	03h36m	−34°58'	8°	38	1436^{+63}_{-36}	286^{+40}_{-29}
M81 Group	09h55m	+69°04'	4°	6	5^{+5}_{-42}	72^{+313}_{-43}
N3184 Group	10h20m	+45°33'	10°:	6	644^{+71}_{-49}	113^{+47}_{-14}
LeoI Group	10h48m	+12°35'	4°	9	749^{+75}_{-48}	130^{+30}_{-16}
Coma clouds	12h20m	+29°17'	15°:	49	907:[e]	234:[e]
N5182 Group	13h25m	−43°01'	20°	15	519^{+24}_{-39}	88^{+22}_{-16}
M101 Group	14h03m	+54°21'	10°	7	225^{+28}_{-45}	111^{+36}_{-19}
N7331 Group	22h37m	+34°25'	10°:	9	911^{+52}_{-86}	123^{+53}_{-15}

[a]Approximate RA and Dec of geometrical center of the group/cluster.

[b]Approximate total extent of the group/cluster.

[c]Number of presumed group members identified in zcat (Huchra & Mader 1998) within the region defined by the previous columns.

[d]Mean heliocentric velocity and velocity dispersion derived using a biweight estimator applied to the velocities tabulated in zcat (Huchra & Mader 1998)

[e]The velocity distribution in the Coma Clouds region is bimodal. Because of uncertain group membership, we give a mean velocity and dispersion for the entire region, rather than for the separate clouds.

Table 6. Summary of Virgo Cluster Sub-Clusters Relevant to this Study

Name	Gal.[a]	RA (B1950)[b]	DEC (B1950)[b]	Diameter[c]	v_{hel}	σ	Reference[d]
			M87 region				
Cluster A	All	$\sim$ 12h26	$\sim$ 13°00	$\sim 1\overset{\circ}{.}6$	1057	710	BTS87
Virgo Cluster (I)	S-Irr	12h27.4m	13°09'	6°	960	780	T85
Virgo Cluster (I)	E+L	12h27.4m	13°09'	6°	1080	510	T85
M87 sub-cluster	All	12h28m	12°40'	2°	1061		H84
Virgo A	All	$\sim$ 12h26m	$\sim$ 13°50'	$\sim 4° \times 8°$	1149	762	G99
Virgo S	All	12h28.6m	13°36'	$\sim$ 6°	991	664	N93
E Cloud	E+L	12h26.5m	13°12'	6°	1000	400	deV73
			NGC 4472 Region				
Southern Cloud (II)	All	12h25m	07°30'	$3\overset{\circ}{.}5$	1240	610	T85
NGC 4472 sub-cluster	All	12h27m	08°17'	2°	1072	···	H84
Cluster B	All	$\sim$ 12h26m	$\sim$ 09°00'	$\sim$ 1°	963	390	BTS87
S-cloud	Sa-Scd	12h27.5m	13°54'	12°	1350	750	deV73
Cloud S	All	$\sim$ 12h31m	$\sim$ 06°20'	$\sim 5\overset{\circ}{.}5 \times 7\overset{\circ}{.}5$	1457	607	G99
Virgo S'	All	12h24.7m	08°12'	$4\overset{\circ}{.}5$	993	371	N93
			NGC 4649 Region				
Cloud E	All	$\sim$ 12h00m	$\sim$ 12°41'	$\sim 3° \times 8°$	1084	702	G99

[a]Galaxy types used in the analysis: S = spirals, E = ellipticals, L = lenticulars, Irr = irregulars.

[b]The groups mean RA and Dec are not tabulated by BTS87 and G99, and have been read from their finding charts.

[c]Approximate diameter of the region covered by the group. The clouds identified by Gavazzi et al. are very elongated, therefore the extension in RA and DEC is given.

[d]BTS87 = Binggeli, Tammann & Sandage 1987, T85 = Tanaka 1985, H84 = Huchra 1985, G99 = Gavazzi et al. 1999, N93 = Nolthenius 1993, deV = de Vaucouleurs & de Vaucouleurs 1973.

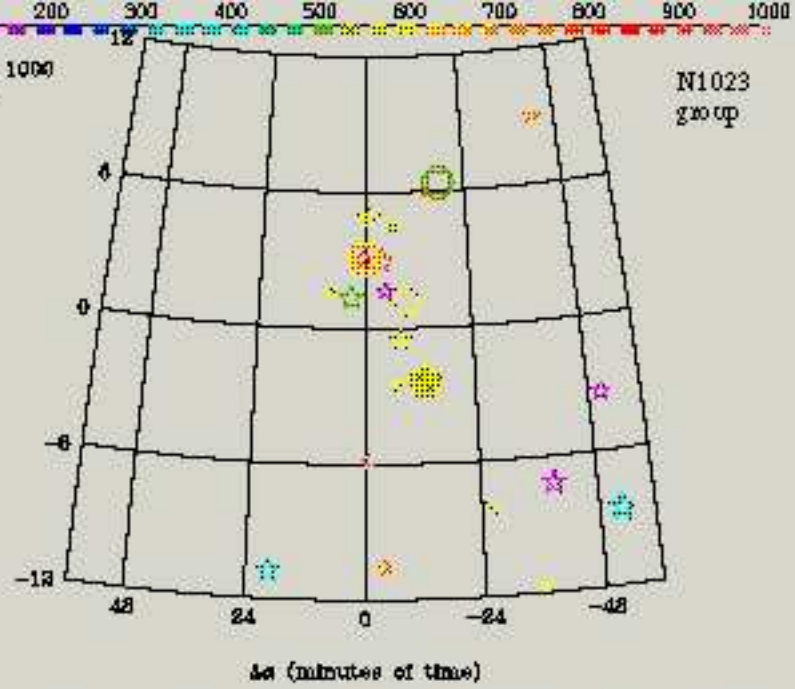
N1023
group
Δα (minutes of time)

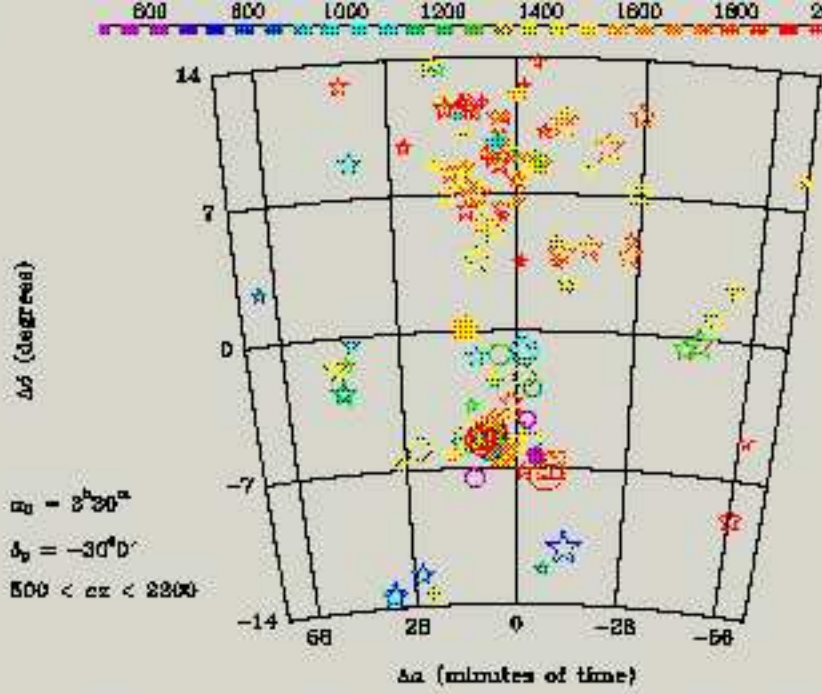
Δδ (degrees)
Δα (minutes of time)

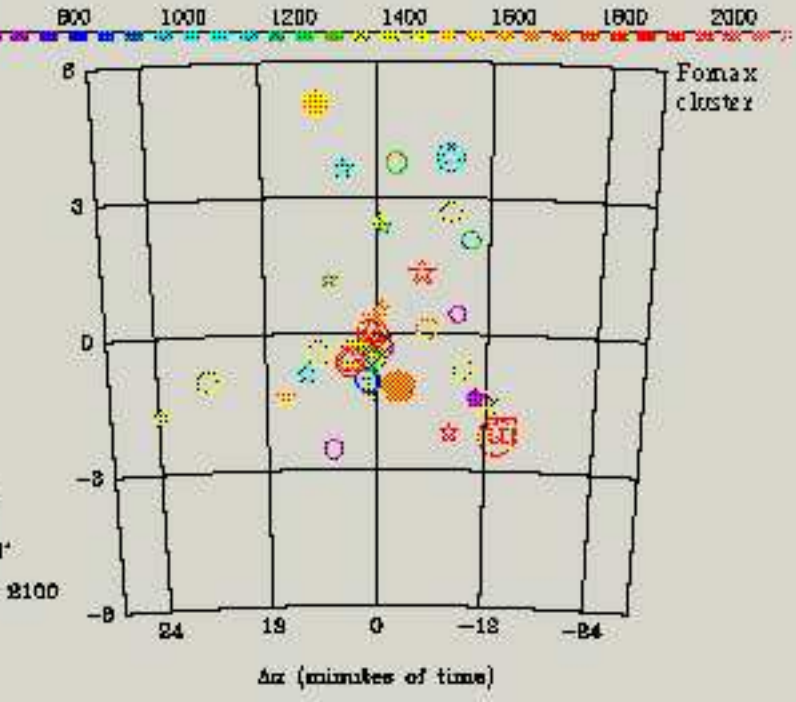
Fornax
cluster
Δα (minutes of time)

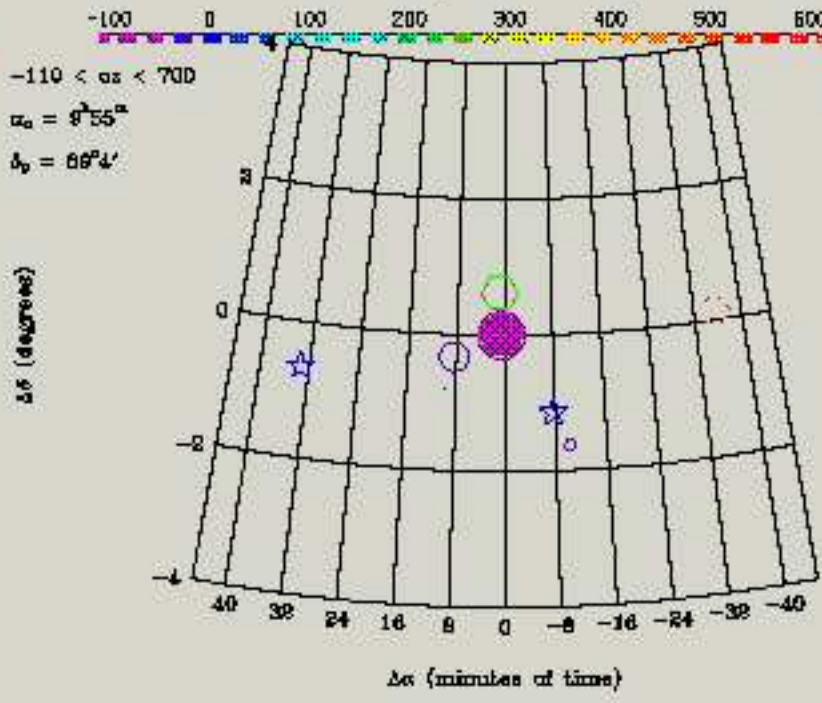
Δδ (degrees)
Δα (minutes of time)

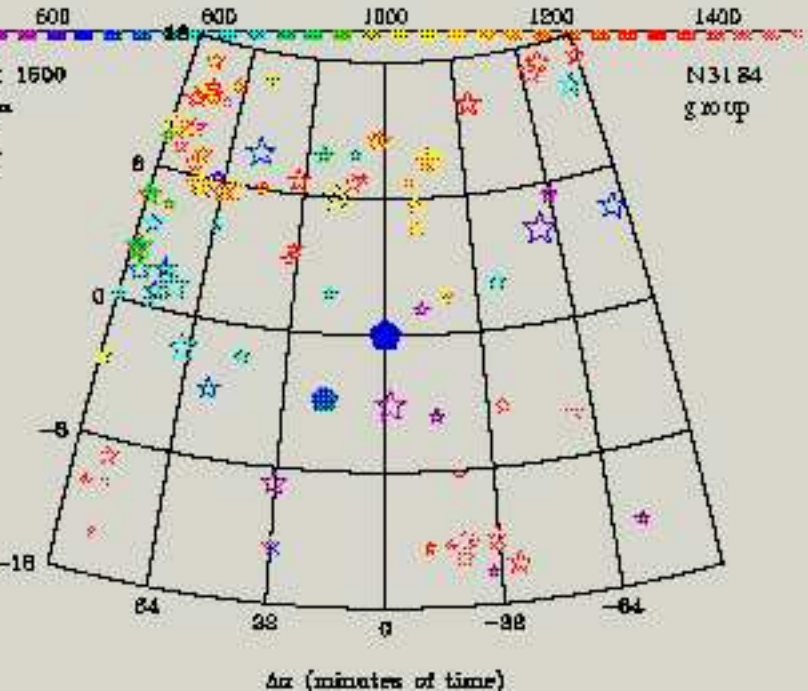
N3184
group
Δα (minutes of time)

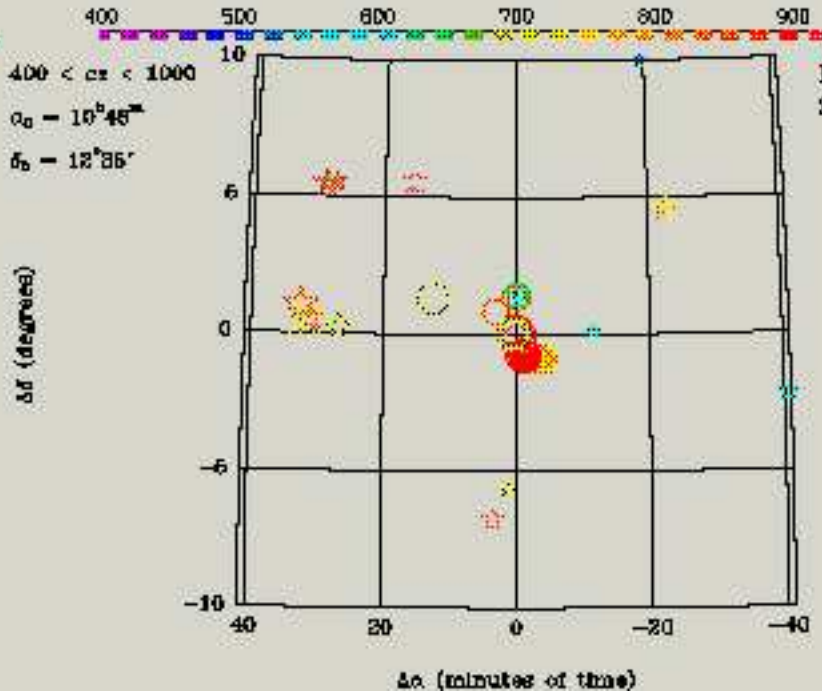
Δδ (degrees)
Δα (minutes of time)

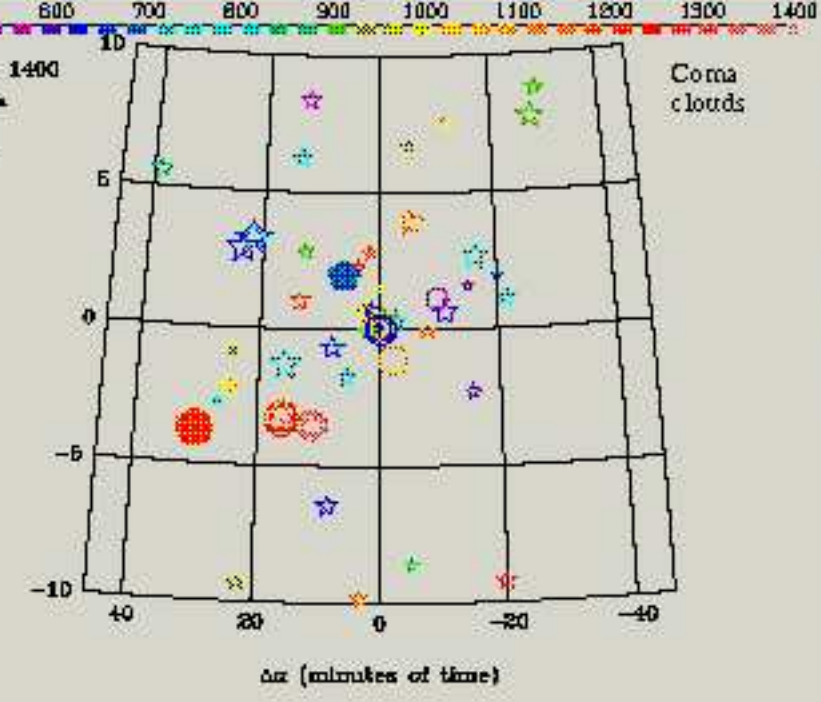
Coma
clouds
Δα (minutes of time)

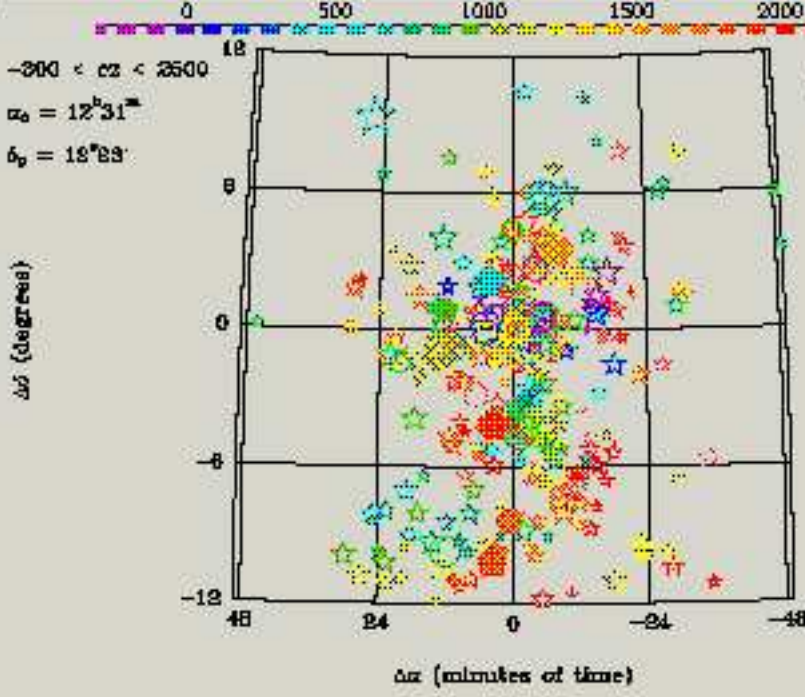
−200 < cz < 2500
Δδ (degrees)
Δα (minutes of time)

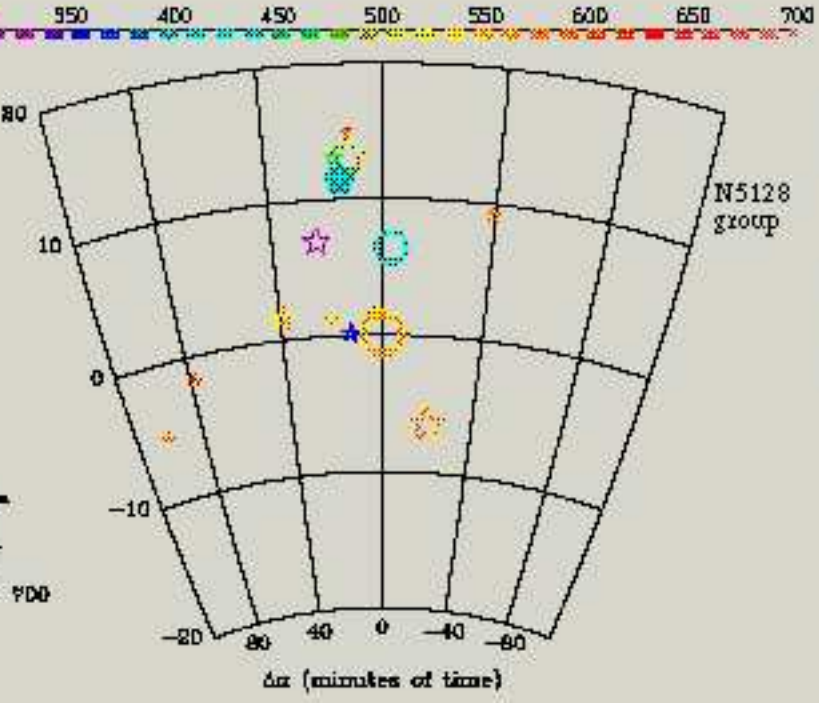
N5128
group
Δα (minutes of time)

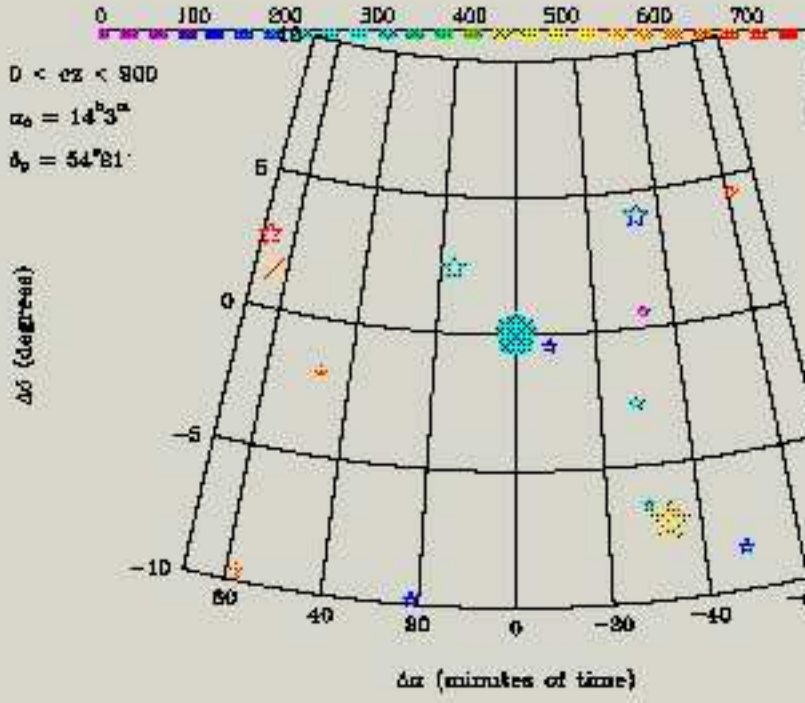
0 < cz < 900
Δδ (degrees)
Δα (minutes of time)

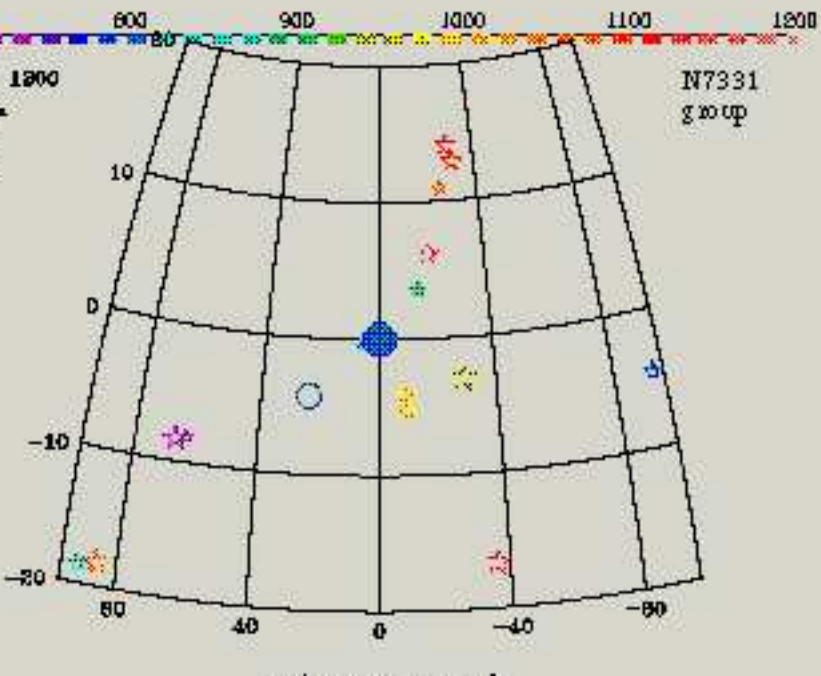
N7331
group

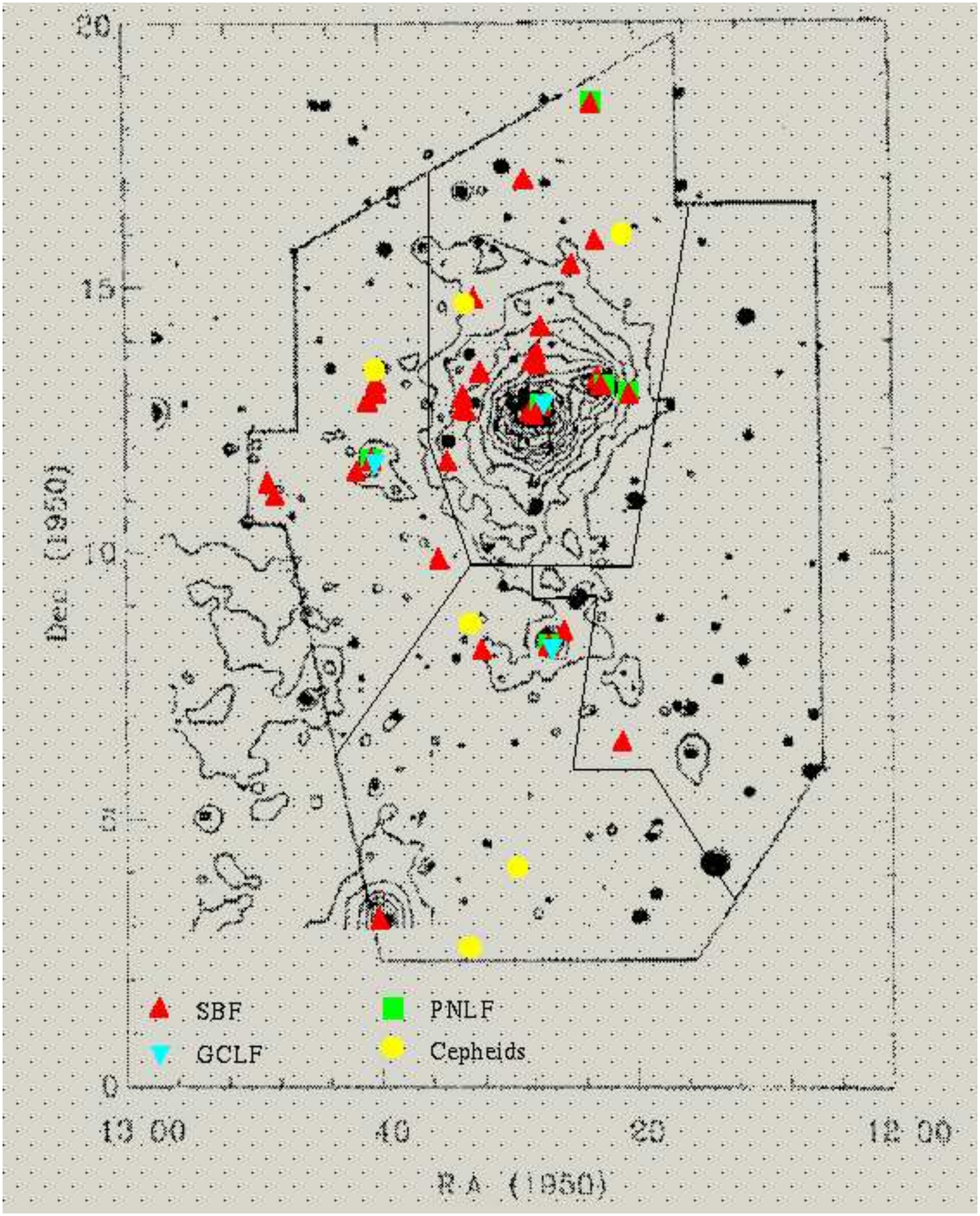
20
15
10
05
0
Dec (1950)
SBF
GCLF
PNLF
Cepheids
13 00
40
20
12 00
R.A. (1950)

Table 2. Reddening, Colors and Metallicity

Galaxy	Reddening $E(B-V)$ Cepheids[a]	DIRBE[b]	HI[c]	Mg_2[d]	GC color [e]	Colors & Metallicity 12+log(O/H)[f]	$(V-I)_{TRGB}$[g,h]	$(V-I)_{-3.5}$[i,h]	$(V-I)_{SBF}$ [j]
WLM	···	0.037	0.022	···	···	7.74±0.50	1.6±0.2	1.4±0.2^{+}	···
IC10	1.16±0.08	0.800[k]	0.800[k]	···	···	8.20±0.50	2.9±0.2^{+}	2.6±0.2^{+}	···
N205	···	0.082	0.034	0.100	···	···	2.0±0.5	1.6±0.3^{+}	···
N221	···	0.068*	0.075	0.185	···	···	···	···	1.241±0.010 (2)
	···	···	···	···	···	···	···	···	1.236±0.007 (1)
N224	0.12±0.12	0.080[l]	0.080[l]	0.308	$B-V=0.8\pm0.1, V-R=0.6\pm0.1$	8.98±0.15	1.97±0.10	1.7±0.1^{+}	1.334±0.007 (1)
	···	···	···	···	···	···	···	···	1.344±0.016 (2)
SMC	0.01±0.05	0.030*	0.041	···	···	7.99±0.08	···	···	···
N300	-0.07±0.03	0.012	0.024	···	···	8.35±0.15	···	···	···
LGS3	···	0.040	0.024	···	···	···	1.31±0.05	1.28±0.05	···
IC1613	0.02	0.025	0.005	···	···	7.86±0.50	1.55±0.26	1.5±0.2^{+}	···
And V dSph	···	0.128	0.160	···	···	···	···	···	···
N598	0.12±0.09	0.042	0.043	···	···	8.82±0.15	1.60±0.10	1.4±0.1^{+}	···
N708	···	0.083	0.056	···	···	···	···	···	1.386±0.020[m]
N891	···	0.065	0.072	···	···	···	···	···	1.225±0.017
N925	0.13±0.02	0.076	0.060	···	···	8.55±0.15	···	···	···
N1023	···	0.060	0.060	0.286	···	···	···	···	1.270±0.017 (1)
	···	···	···	···	···	···	···	···	1.314±0.012 (2)
N1316	···	0.021	0.000	···	···	···	···	···	1.159±0.016
N1326A	0.00±0.01	0.016	0.000	···	···	8.50±0.15	···	···	···
N1339	···	0.013	0.000	···	···	···	···	···	1.152±0.012
N1344	···	0.018	0.000	0.263	···	···	···	···	1.159±0.011
N1365	0.15±0.03	0.010	0.000	···	···	8.96±0.20	···	···	···
N1379	···	0.012	0.000	0.257	$V-I$=1.17±0.03, $B-I=1.6\pm0.2$	···	···	···	1.158±0.019
N1380	···	0.017	0.000	···	$B-V=0.71\pm0.14, V-R=0.51\pm0.14$ (4)	···	···	···	1.221±0.019
N1399	···	0.013	0.000	0.334	$C-T_1=1.51\pm0.03$ (5)	···	···	···	1.245±0.014
N1395	···	0.023	0.005	0.313	···	···	···	···	1.245±0.010
N1404	···	0.007	0.000	0.317	$V-R$=0.51±0.1 (7)	···	···	···	1.239±0.016
N1400	···	0.065	0.031	0.309	···	···	···	···	1.253±0.009
N1407	0.10±0.06	0.068	0.039	0.327	···	···	···	···	1.311±0.010
N1425	0.07±0.03	0.013	0.000	···	···	9.00±0.15	···	···	···
N1426	···	0.016	0.005	0.276	···	···	···	···	1.182±0.009
LMC	0.10	0.100[n]	0.100[n]	···	···	8.50±0.08	1.8±0.2	1.6±0.3^{+}	···
N2090	0.07±0.01	0.040	0.000	···	···	8.80±0.15	···	···	···
N2403	N/A	0.062[o]	0.039[o]	···	···	8.80±0.10	···	···	···
N2366	N/A	0.036	0.041	···	···	7.96±0.50	···	···	···

Table 2—Continued

Galaxy	Reddening $E(B-V)$ Cepheids[a]	DIRBE[b]	HI[c]	Mg_2[d]	GC color [e]	Colors & Metallicity 12+log(O/H)[f]	$(V-I)_{TRGB}$[g,h]	$(V-I)_{-3.5}$[i,h]	$(V-I)_{SBF}$ [j]
N2541	0.08±0.05	0.050	0.041	···	···	8.50±0.15	···	···	···
U4305	N/A	0.032	0.021	···	···	7.87±0.06	···	···	···
F8DI	···	0.100	0.048	···	···	···	1.85±0.04	1.650±0.012	···
N3031	0.03	0.080[p]	0.034[p]	···	···	8.75±0.15	···	···	1.290±0.011
N3034	···	0.159	0.036	···	···	···	$1.9\pm0.3^{+}$	$1.5\pm0.3^{+}$	···
Leo A	···	0.021	0.017	···	···	7.30±0.37	$1.3\pm0.2^{+}$	$1.2\pm0.2^{+}$	···
Sextans B	0.02	0.031	0.012	···	···	7.56±0.50	1.4±0.2	$1.4\pm0.3^{+}$	···
N3109	0.18:±0.08	0.058	0.034	···	···	8.06±0.15	1.7±0.2	1.41±0.07 (14)	···
	···	···	···	···	···	···	1.45±0.3	1.35±0.30 (89)	···
BK5N	···	0.064	0.032	···	···	···	1.55±0.06	1.425±0.015	···
N3115	···	0.047	0.024	0.309	···	···	2.0±0.2	$1.5\pm0.2^{+}$	1.242±0.010
N3115DW1	···	0.052	0.041	···	$B-V$ =0.76±0.03	···	···	···	···
Leo I	···	0.037	0.023	···	···	···	$1.4\pm0.1^{+}$	$1.2\pm0.1^{+}$	···
Sextans A	0.05±0.05	0.044	0.014	···	···	7.49±0.54	1.5±0.2	$1.3\pm0.4^{+}$	···
N3198	0.05±0.03	0.012	0.000	···	···	8.60±0.15	···	···	···
N3319	0.04±0.03	0.015	0.000	···	···	8.38±0.15	···	···	···
N3351	0.11	0.028	0.010	···	···	9.24±0.20	···	···	···
N3368	0.14±0.04	0.025	0.012	···	···	9.20±0.20	···	···	1.178±0.015
N3377	···	0.033	0.014	0.270	···	···	···	···	1.158±0.009 (1)
	···	···	···	···	···	···	···	···	1.225±0.003 (2)
N3379	···	0.024	0.012	0.308	···	···	N/A	N/A	1.223±0.015 (1)
	···	···	···	···	···	···	···	···	1.261±0.006 (5)
	···	···	···	···	···	···	···	···	1.261±0.006 (2)
N3384	···	0.026	0.017	···	···	···	···	···	1.184±0.018 (1)
	···	···	···	···	···	···	···	···	1.231±0.005 (2)
Leo B	···	0.017	0.000	···	···	···	1.48±0.07	1.28±0.06	···
N3621	0.22±0.02	0.081	0.094	···	···	8.75±0.15	···	···	···
N3627	0.14±0.04	0.032	0.002	···	···	9.25±0.15	···	···	···
N4278	···	0.028	0.024	0.291	···	···	···	···	1.196±0.012
N4321	0.13±0.08	0.026	0.012	···	···	9.13±0.20	···	···	···
N4365	···	0.021	0.000	0.321	$V-I$=1.09 (19)	···	···	···	1.249±0.017
N4374	···	0.041	0.029	0.305	···	···	···	···	1.241±0.008
N4373	···	0.078	0.093	0.292	···	···	···	···	1.252±0.023 (1)
	···	···	···	···	···	···	···	···	1.292±0.042 (5)
N4382	···	0.031	0.007	0.227	···	···	···	···	1.188±0.022
N4406	···	0.029	0.027	0.311	···	···	···	···	1.205±0.008 (1)

Table 2—Continued

Galaxy	Reddening $E(B-V)$ Cepheids[a]	DIRBE[b]	HI[c]	Mg_2[d]	GC color [e]	Colors & Metallicity 12+log(O/H)[f]	$(V-I)_{TRGB}$[g,h]	$(V-I)_{-3.5}$[i,h]	$(V-I)_{SBF}$ [j]
	···	···	···	···	···	···	···	···	1.256±0.011 (5)
	···	···	···	···	···	···	···	···	1.256±0.011 (2)
N4414	0.01±0.04	0.019	0.005	···	···	9.20±0.15	···	···	···
IC3388	···	0.021	0.019	···	···	···	N/A	N/A	···
N4458	···	0.024	0.017	0.227	···	···	···	···	1.170±0.011 (1)
	···	···	···	···	···	···	···	···	1.192±0.010 (2)
N4472	···	0.022	0.000	0.314	$C-T_1 = 1.527 \pm 0.07$ (15)	···	···	···	1.248±0.011 (1)
	···	···	···	···	···	···	···	···	1.292±0.012 (2)
N4473	···	0.028	0.014	0.304	···	···	···	···	1.193±0.012 (1)
	···	···	···	···	···	···	···	···	1.261±0.009 (2)
N4478	···	0.024	0.022	0.249	···	···	···	···	1.197±0.019 (1)
N4486	···	0.023	0.022	0.289	···	···	···	···	1.274±0.012
N4489	···	0.027	0.005	0.198	···	···	···	···	1.081±0.015
N4494	···	0.021	0.012	0.275	···	···	···	···	1.166±0.010
N4496A	0.04±0.02	0.025	0.002	···	···	8.77±0.15	···	···	···
IG Stars	···	0.031	0.022	···	···	···	N/A	N/A	···
N4535	0.10±0.03	0.019	0.000	···	···	9.20±0.15	···	···	···
N4536	0.10±0.02	0.018	0.000	···	···	8.85±0.15	···	···	···
N4548	0.09±0.02	0.038	0.014	···	···	9.34±0.15	···	···	1.195±0.019
N4552	···	0.041	0.034	0.324	···	···	···	···	1.247±0.015 (1)
	···	···	···	···	···	···	···	···	1.308±0.010 (2)
N4565	···	0.015	0.007	···	···	···	···	···	1.149±0.027
N4571	N/A	0.048	0.012	···	···	···	···	···	···
N4578	···	0.021	0.000	···	···	···	···	···	1.154±0.015
N4594	···	0.051	0.029	0.330	···	···	···	···	1.240±0.031 (1)
	···	···	···	···	···	···	···	···	1.289±0.014 (2)
N4603	···	0.168	0.123	···	···	···	···	···	···
N4621	···	0.032	0.014	0.328	···	···	···	···	1.213±0.018 (1)
	···	···	···	···	···	···	···	···	1.287±0.013 (2)
N4636	···	0.028	0.012	0.311	···	···	···	···	1.268±0.011
N4639	0.05±0.03	0.026	0.012	···	···	9.0±0.15	···	···	···
N4649	···	0.027	0.010	0.338	···	···	···	···	1.267±0.023 (1)
	···	···	···	···	···	···	···	···	1.323±0.004 (2)
N4660	···	0.035	0.000	0.297	···	···	···	···	1.195±0.015 (1)
	···	···	···	···	···	···	···	···	1.250±0.015 (2)
N4725	0.19±0.03	0.012	0.007	···	···	8.92±0.15	···	···	1.224±0.023

Table 2—Continued

Galaxy	Reddening $E(B-V)$ Cepheids[a]	DIRBE[b]	HI[c]	Mg_2[d]	GC color [e]	Colors & Metallicity 12+log(O/H)[f]	$(V-I)_{TRGB}$[g,h]	$(V-I)_{-3.5}$[i,h]	$(V-I)_{SBF}$ [j]
GR8	N/A	0.025	0.010	···	···	7.43±0.48	···	···	···
N4881	···	0.011	0.015	0.293	···	···	···	···	···
IC4051	···	0.011	0.012	0.337	$V-I$=1.08±0.01	···	···	···	···
IC4182	-0.03±0.03	0.014	0.000	···	···	8.40±0.20	···	···	···
N5102	···	0.055	0.048	0.005	···	···	···	···	1.047±0.016
N5128	···	0.115	0.118	···	···	···	$1.9\pm0.2^{+}$	$1.7\pm0.2^{+}$	1.226±0.010
N5170	···	0.078	0.051	···	···	···	···	···	···
N5195	···	0.036	0.000	···	···	···	···	···	1.103±0.019
N5193	···	0.057	0.030	···	···	···	···	···	1.278±0.020[m]
IC4296	···	0.060	0.030	0.321	···	···	···	···	1.275±0.020[m]
N5253	0.14±0.05	0.056	0.046	···	···	8.15±0.15	···	···	···
N5457	0.13	0.009[q]	0.000[q]	···	···	9.05±0.15	···	···	···
N5481	···	0.019	0.002	···	$B-V$=0.8±0.8, $V-R$=0.6±0.6	···	···	···	···
N5846	···	0.056	0.034	0.321	$V-I$=1.21	···	···	···	1.298±0.007
N6822	0.24±0.03	0.236	0.207	···	···	8.25±0.07	2.0±0.2	1.4±0.2	···
N7014	···	0.033	0.018	···	···	···	···	···	1.290±0.020[m]
N7331	0.14±0.05	0.091	0.080	0.214	···	8.67±0.15	···	···	1.235±0.017
N7457	···	0.051	0.051	0.159	···	···	···	···	1.172±0.009 (1)
	···	···	···	···	···	···	···	···	1.209±0.020 (2)
UKS2323−326	···	0.015	···	···	···	···	1.43±0.05	1.29±0.04	···
Cassiopeia	···	0.197	···	···	···	···	$1.9\pm0.1^{+}$	1.46±0.01	···
And VI	···	0.063	···	···	···	···	1.83±0.20 (2)	1.53±0.20 (2)	···
	···	···	···	···	···	···	$1.7\pm0.1^{+}$(3)	1.64±0.02 (3)	···

[a]Internal plus galactic $E(B-V)$ in magnitudes, estimated from multiband observations of Cepheid variables. The references are as in column 5 of Table 3.

[b]Galactic $E(B-V)$ in magnitudes, estimated from DIRBE/IRAS 100 μm maps obtained on line from http://star−www.dur.ac.uk:80/∼schlegel/dust/index.html. The 1σ error on the $E(B-V)$ values is 16% (Schlegel et al. 1998). For galaxies marked by a *, the extended IRAS source has not been properly subtracted from the maps, therefore $E(B-V)$ has been determined as the mean of the two points at the same galactic latitude as the galaxy, and 3° away in longitude from the center, and on either side.

[c]Galactic $E(B-V) = A_B/4.0$ in magnitudes, from Burstein & Heiles (1984). Typical error on $E(B-V)$ is ± 0.015 mag.

[d]Mg2 index from Faber et al. (1989); Bender, Burstein & Faber (1993); Gorgas, Efstathiou & Aragón Salamanca 1990; Huchra et al. 1996; Golev et al. 1999.

[e]Mean Globular Cluster color corresponding to the peak of the GC luminosity function. References are given in Table 3, column 10, and are repeated here in parenthesis whenever confusion might arise. The color distribution for NGC 3115 and NGC 4486 is bimodal, and is not quoted in this paper.

[f]Metallicity of HII regions, defined as [O/H]=log(O/H)/$(\mathrm{O/H})_\odot$, with $(\mathrm{O/H})_\odot = 7.9 \times 10^{-4}$. The references are: SMC and LMC Pagel et al. (1978); GR8 Skillman et a. (1988); Leo A, WLM, IC 1613, Sextans A and Sextans B Skillman et al. (1989); UGC4305 Masegosa et al. (1991); NGC 6822 Pagel et al. (1980); IC 10 Lequeux et al. (1979); M101 Kennicutt et al. (1998); NGC 1326A, NGC 1425, NGC 2090, NGC 4414, NGC 4496A, NGC 4535, NGC 4536, NGC 4548, NGC 4639 and IC 4182 Kennicutt (1999) M31, M33, M81, N300, N925, N1365, N3351 and N4321 Zaritsky et al. (1994); N3109 Richer & McCall (1995); N3368 Oey & Kennicutt (1993); N5253 Webster & Smith (1983).

[g]$V-I$ color of the tip of the red giant branch. References are given in column 11 of Table 3.

[h]The $V-I$ color is not corrected for either internal nor galactic extinction. For NGC 3115 the quoted values have been calculated from the published unreddened values using the extinction given by the authors ($A_I = 0.05$). $V-I$ colors are not explicitly quoted for the numbers flagged by a $^+$, in which case we have measured the colors from the published color magnitude diagrams.

[i]$V-I$ color measured at an absolute I magnitude of -3.5 (~ 0.5 mag below the tip of the RGB). References are given in column 11 of Table 3, and are repeated here in parenthesis whenever confusion might arise.

[j]Galaxy color determined from the SBF measurements, referenced in column 14 of Table 3. The reference is repeated here in parenthesis whenever confusion might arise. In all cases, the colors are not corrected for either internal or Galactic extinction. Published dereddened values have been corrected using the extinction given by the authors.

[k]Extinction derived from Wolf−Rayet stars by Massey & Armandroff (1995). See also Sakai, Madore & Freedman for a comprehensive discussion

[l]Extinction derived from various sources, see Bianchi et al. (1996) for an extensive review.

[n]The value quoted is from measurements of the Balmer decrement in several PNe, estimates from B stars, star clusters and HI measurements. See Jacoby, Walker & Ciardullo (1990) for a complete discussion. For comparison, DIRBE/IRAS and HI measurements give $E(B-V) = 0.075$, and $E(B-V) = 0.060$ respectively.

[o]Humphreys et al. (1986) report a total extinction estimate $E(B-V) \sim 0.09$ from M supergiants, implying little internal extinction.

[p]Estimates of the total extinction in M81 are from Kaufman et al. (1987) who find $E(B-V) \sim 0.10$ from the study of giant HII regions, and Humphreys et al. (1986) who find $E(B-V) \sim 0.2$ from M supergiants. Because our distance indicators are largely little affected by internal extinction, we prefer to adopt only the foreground estimates given in the table.

[q]Humphreys et al. (1986) report a total extinction estimate $E(B-V) \sim 0.15$ from M supergiants

Table 3. Cepheid Distance Moduli and TRGB, PNLF, GCLF & SBF Characteristic Magnitudes to Individual Galaxies

	Cepheids				TRGB		PNLF			GCLF			SBF	
Galaxy	No[a]	Bands	$(m-M)\pm\sigma$ [b]	Ref[c]	$I_{TRGB}\pm\sigma$ [d]	Ref [e]	No[f]	$m^*_{5007}\pm\sigma$ [g]	Ref [h]	$m_T\pm\sigma$ [i]	Ref [j]	$\overline{m}\pm\sigma$ [k]	Ref [l]
Local Group													
And V	···	···	···	···	20.85±0.10	1	···	···	···	···	···	···	···
And VI	···	···	···	···	20.58±0.20	2	···	···	···	···	···	···	···
	···	···	···	···	20.7±0.1	3	···	···	···	···	···	···	···
Cassiopeia	···	···	···	···	20.7±0.1	3	···	···	···	···	···	···	···
UKS2323−326	···	···	···	···	22.65±0.10	4	···	···	···	···	···	···	···
GR8	1	r	≤26.8:	1	···	···	···	···	···	···	···	···	···
IC10	4	VIJHK	24.10±0.19	2	21.70±0.15	5	···	···	···	···	···	···	···
IC1613	25	BVRI	24.42±0.13	3	20.25±0.15	6	···	···	···	···	···	···	···
LeoI	···	···	···	···	18.0±0.1	7	···	···	···	···	···	···	···
LeoA	···	···	···	···	20.5±0.2	8	···	···	···	···	···	···	···
LeoB	···	···	···	···	17.7±0.2	9	···	···	···	···	···	···	···
LGS3	···	···	···	···	20.6±0.2	10	···	···	···	···	···	···	···
LMC	N/A	N/A	18.50±0.13[m]	3	14.60±0.09	11	42	14.32±0.10	1	···	···	···	···
N205	···	···	···	···	20.4±0.2	12	12	20.41±0.80	2	···	···	···	···
N221	···	···	···	···	···	···	9	20.5 ±1.1	2	···	···	I =22.88±0.05	1
	···	···	···	···	···	···	···	···	···	···	···	F814W=22.99±0.03	2
	···	···	···	···	···	···	···	···	···	···	···	K'=18.56±0.09	3
N224	38	BVRI	24.44±0.10	3	20.55±0.17	13	104	20.17±0.09	2	V =17.00±0.15	1	I =23.18±0.05	1
	···	···	···	···	···	···	···	···	···	···	···	F814W=23.69±0.016	2
	···	···	···	···	···	···	···	···	···	···	···	K'=18.82±0.09	3
N598	10	BVRI	24.64±0.09	4	20.95±0.17	13	···	···	···	···	···	···	···
N3109	4	BVRI	25.26±0.22	5	21.55±0.10	14	N/A	≤ 21.9:±0.4[n]	3	···	···	···	···
	···	···	···	···	21.70±0.06	15	···	···	···	···	···	···	···
N6822	8	BVRI	23.49±0.09	6	19.80±0.10	16	···	···	···	···	···	···	···
SextansA	5	BVRI	25.85±0.15	7	21.73±0.09	17	···	···	···	···	···	···	···
SextansB	8	BVRI	25.69±0.25	8	21.60±0.10	18	···	···	···	···	···	···	···
SMC	91	JHK	18.99±0.05	9	···	···	8	14.82:±0.30	1	···	···	···	···
WLM	···	···	···	···	20.85±0.10	19	···	···	···	···	···	···	···
NGC 1023 Group													
N891	···	···	···	···	···	···	34	25.76±0.10	4	···	···	I =27.96±0.11	1
N925	80	VI	29.84±0.08	10	···	···	···	···	···	···	···	···	···
N1023	···	···	···	···	···	···	97	25.71±0.07	4	···	···	I =28.86±0.13	1
	···	···	···	···	···	···	···	···	···	···	···	F814W=29.23±0.04	2
Fornax Cluster													
N1316	···	···	···	···	···	···	58	26.65±0.08	5	···	···	I =29.87±0.15	1

Table 3—Continued

	Cepheids				TRGB		PNLF			GCLF		SBF	
Galaxy	No[a]	Bands	$(m-M)\pm\sigma$ [b]	Ref[c]	$I_{TRGB}\pm\sigma$ [d]	Ref [e]	No[f]	$m^*_{5007}\pm\sigma$ [g]	Ref [h]	$m_T\pm\sigma$ [i]	Ref [j]	$\overline{m}\pm\sigma$ [k]	Ref [l]
N1326A	8	VI	31.43±0.07[t]	11	···	···	···	···	···	···	···	···	···
N1339	···	···	···	···	···	···	···	···	···	···	···	I =29.82±0.35	1
	···	···	···	···	···	···	···	···	···	···	···	K'=25.96:±0.15	3
N1344	···	···	···	···	···	···	···	···	···	V =23.80±0.25	2	I =29.71±0.29	1
	···	···	···	···	···	···	···	···	···	···	···	K'=25.58±0.12	3
N1365	26	VI	31.39±0.10[t]	12	···	···	···	···	···	···	···	···	···
N1379	···	···	···	···	···	···	···	···	···	B =24.95±0.30	3	I =29.76±0.11	1
	···	···	···	···	···	···	···	···	···	···	···	K'=25.44±0.13	3
N1380	···	···	···	···	···	···	···	···	···	V =24.05±0.25	2	I =29.83±0.15	1
	···	···	···	···	···	···	···	···	···	V =23.67±0.11	4	···	···
N1399	···	···	···	···	···	···	37	26.69±0.08	5	V =23.83±0.15	2	I =30.14±0.13	1
	···	···	···	···	···	···	···	···	···	V =23.71±0.12[o]	5	K'=25.98±0.16	3
	···	···	···	···	···	···	···	···	···	B =24.59±0.10	6	···	
N1404	···	···	···	···	···	···	19	26.67±0.10	5	V =24.10±0.20	7	I =30.22±0.16	1
	···	···	···	···	···	···	···	···	···	V =23.92±0.20	2	K'=25.82±0.14	3
	···	···	···	···	···	···	···	···	···	B =24.86±0.21	6	···	···
N1425	20	VI	31.81±0.06[t]	13	···	···	···	···	···	···	···	···	···
Eridanus Cluster													
N1395	···	···	···	···	···	···	···	···	···	···	···	I =30.52±0.14	1
	···	···	···	···	···	···	···	···	···	···	···	K'=25.43:±0.17	3
N1400	···	···	···	···	···	···	···	···	···	···	···	I =30.59±0.32	1
	···	···	···	···	···	···	···	···	···	···	···	K'=26.47:±0.25	3
N1407	···	···	···	···	···	···	···	···	···	···	···	I =31.02±0.25	1
	···	···	···	···	···	···	···	···	···	···	···	K'=26.20±0.15	3
N1426	···	···	···	···	···	···	···	···	···	···	···	I =30.25±0.17	1
	···	···	···	···	···	···	···	···	···	···	···	K'=25.67:±0.30	3
M81 Group													
N2366	6	r	≤27.7:	14	···	···	···	···	···	···	···	···	···
N2403	17	I	≤27.5:	1	···	···	···	···	···	···	···	···	···
N3031	30	VI	27.80±0.08	15	···	···	89	23.60±0.08	6	V=20.9:±0.5	8	I =26.54±0.25	1
N3034	···	···	···	···	23.95±0.14	20	···	···	···	···	···	···	···
BK5N	···	···	···	···	23.95±0.11	21	···	···	···	···	···	···	···
F8DI	···	···	···	···	24.00±0.07	21	···	···	···	···	···	···	···
U4305	7	r	≤27.42:	16	···	···	···	···	···	···	···	···	···
NGC 3184 Group													
N3198	58	VI	30.80±0.06	17	···	···	···	···	···	···	···	···	···

Table 3—Continued

Galaxy	Cepheids No[a]	Bands	$(m-M)\pm\sigma$ [b]	Ref[c]	TRGB $I_{TRGB}\pm\sigma$ [d]	Ref [e]	PNLF No[f]	$m^*_{5007}\pm\sigma$ [g]	Ref [h]	GCLF $m_T\pm\sigma$ [i]	Ref [j]	SBF $\overline{m}\pm\sigma$ [k]	Ref [l]
N3319	28	VI	30.78±0.10	18	···	···	···	···	···	···	···	···	···
Leo I Group													
N3351	49	VI	30.01±0.08	19	···	···	···	···	···	···	···	···	···
N3368	7	VI	30.20±0.10[u]	20	···	···	25	25.42±0.10	7	···	···	I =28.37±0.20	1
N3377	···	···	···	···	···	···	22	25.64±0.18	8	···	···	I =28.42±0.06	1
	···	···	···	···	···	···	···	···	···	···	···	F814W=28.62±0.05	2
N3379	···	···	···	···	26.32±0.09	22	45	25.52±0.13	8	B =22.70±0.25	9	I =28.62±0.07	1
	···	···	···	···	···	···	···	···	···	···	···	$F814W$ =28.89±0.11	4
	···	···	···	···	···	···	···	···	···	···	···	F814W=29.04±0.05	2
	···	···	···	···	···	···	···	···	···	···	···	K_s=24.48±0.09	5
N3384	···	···	···	···	···	···	43	25.61±0.13	8	···	···	I =28.64±0.10	1
	···	···	···	···	···	···	···	···	···	···	···	F814W=28.90±0.02	2
N3627	17	VI	30.06±0.17[u]	20	···	···	···	···	···	···	···	···	···
Coma I Cloud													
N4278	···	···	···	···	···	···	23	25.65±0.16	9	V =23.23±0.12	10	I =29.39±0.18	1
N4414	9	VI	31.41±0.10	21	···	···	···	···	···	···	···	···	···
Coma II Cloud													
N4494	···	···	···	···	···	···	101	26.11±0.06	9	V =23.07±0.14	10	I =29.42±0.08	1
	···	···	···	···	···	···	···	···	···	V =23.32±0.35	11	···	···
N4565	···	···	···	···	···	···	17	25.68±0.14	9	V =22.63±0.20	11	I =29.40±0.11	1
N4725	13	VI	30.57±0.08[t]	22	···	···	···	···	···	···	···	I =29.16±0.32	1
M87 sub−cluster in the Virgo cluster													
IC3388	···	···	···	···	26.82±0.07	23	···	···	···	···	···	···	···
IG Stars	···	···	···	···	27.44±0.30	24	···	···	···	···	···	···	···
N4321	42	VI	31.04±0.09	23	···	···	···	···	···	···	···	···	···
N4374	···	···	···	···	···	···	37	26.56±0.13	10	···	···	I =29.85±0.09	1
	···	···	···	···	···	···	···	···	···	···	···	K_s=25.43±0.22	5
N4382	···	···	···	···	···	···	59	26.37±0.12	10	···	···	I =29.65±0.09	1
N4406	···	···	···	···	···	···	59	26.56±0.11	10	···	···	I =29.67±0.06	1
	···	···	···	···	···	···	···	···	···	···	···	F814W=29.91±0.02	4
	···	···	···	···	···	···	···	···	···	···	···	F814W=30.06±0.05	2
	···	···	···	···	···	···	···	···	···	···	···	K'=25.46±0.10	3
N4458	···	···	···	···	···	···	···	···	···	···	···	I =29.37±0.21	1
	···	···	···	···	···	···	···	···	···	···	···	F814W=29.31±0.06	2
N4473	···	···	···	···	···	···	···	···	···	···	···	I =29.33±0.11	1
	···	···	···	···	···	···	···	···	···	···	···	F814W=29.79±0.07	2

Table 3—Continued

Galaxy	Cepheids No[a]	Bands	$(m-M)\pm\sigma$ [b]	Ref[c]	TRGB $I_{TRGB}\pm\sigma$ [d]	Ref [e]	PNLF No[f]	$m^*_{5007}\pm\sigma$ [g]	Ref [h]	GCLF $m_T\pm\sigma$ [i]	Ref [j]	SBF $\overline{m}\pm\sigma$ [k]	Ref [l]
N4478	···	···	···	···	···	···	···	···	···	V=23.82±0.38	12	I =29.67±0.26	1
	···	···	···	···	···	···	···	···	···	···	···	F814W=29.78:±0.10	6
	···	···	···	···	···	···	···	···	···	···	···	K_s=25.24±0.13	5
N4486	···	···	···	···	···	···	187	26.33±0.10	11	V =23.74±0.07	13	I =29.89±0.11	1
N4489	···	···	···	···	···	···	···	···	···	···	···	I=29.10±0.13	1
	···	···	···	···	···	···	···	···	···	···	···	K_s=23.56:±0.22	5
	···	···	···	···	···	···	···	···	···	···	···	K'=24.99±0.35	3
N4548	26	VI	31.04±0.08	24	···	···	···	···	···	···	···	I =29.74±0.53	1
N4552	···	···	···	···	···	···	···	···	···	···	···	I =29.47±0.11	1
	···	···	···	···	···	···	···	···	···	···	···	K_s=24.86±0.06	5
	···	···	···	···	···	···	···	···	···	···	···	F814W=29.86±0.07	2
	···	···	···	···	···	···	···	···	···	···	···	K'=25.45±0.11	3
N4571	3	R	≤30.9:	25	···	···	···	···	···	···	···	···	···
NGC 4472 sub−cluster in the Virgo cluster													
N4472	···	···	···	···	···	···	26	26.29±0.13	10	B =24.78±0.23	14	I =29.67±0.07	1
	···	···	···	···	···	···	···	···	···	V =23.77±0.11[p]	15	F814W=30.09±0.04	2
	···	···	···	···	···	···	···	···	···	···	···	K_s=25.25±0.13	5
	···	···	···	···	···	···	···	···	···	···	···	K'=25.30±0.11	3
N4496A	51	VI	31.02±0.07[u]	20	···	···	···	···	···	···	···	···	···
N4535	25	VI	31.10±0.07[t]	26	···	···	···	···	···	···	···	···	···
N4536	27	VI	30.95±0.07[u]	20	···	···	···	···	···	···	···	···	···
N4636	···	···	···	···	···	···	···	···	···	···	···	I =29.51±0.11	1
	···	···	···	···	···	···	···	···	···	···	···	K_s=24.79±0.11	5
	···	···	···	···	···	···	···	···	···	···	···	K'=25.59±0.15	3
NGC 4649 sub−cluster in the Virgo cluster													
N4578	···	···	···	···	···	···	···	···	···	···	···	I =29.54±0.10	1
	···	···	···	···	···	···	···	···	···	···	···	K'=25.54:±0.30	3
N4621	···	···	···	···	···	···	···	···	···	···	···	I =29.73±0.18	1
	···	···	···	···	···	···	···	···	···	···	···	F814W=29.63±0.05	2
	···	···	···	···	···	···	···	···	···	···	···	K_s=25.41±0.16	5
N4639	17	VI	31.80±0.09[u]	20	···	···	···	···	···	···	···	···	···
N4649	···	···	···	···	···	···	16	26.34±0.13	10	B =24.47±0.18	14	I =29.81±0.09	1
	···	···	···	···	···	···	···	···	···	···	···	F814W=30.20±0.06	2
N4660	···	···	···	···	···	···	···	···	···	···	···	I =28.88±0.17	1
	···	···	···	···	···	···	···	···	···	···	···	F814W=29.37±0.13	2
NGC 5128 Group													

Table 3—Continued

Galaxy	Cepheids No[a]	Bands	$(m-M)\pm\sigma$ [b]	Ref[c]	TRGB $I_{TRGB}\pm\sigma$ [d]	Ref [e]	PNLF No[f]	$m^*_{5007}\pm\sigma$ [g]	Ref [h]	GCLF $m_T\pm\sigma$ [i]	Ref [j]	SBF $\overline{m}\pm\sigma$ [k]	Ref [l]
N5102	···	···	···	···	···	···	19	23.17±0.21	12	···	···	I =25.60±0.09	1
N5128	···	···	···	···	24.1±0.1	25	224	23.61±0.07	13	···	···	I =26.28±0.11	1
N5253	7	VI	27.61±0.11[u]	20	···	···	16	23.76:±0.40	14	···	···	···	···
M101 Group													
N5195	···	···	···	···	···	···	38	25.08±0.10	7	···	···	I =27.32±0.25	1
N5457[q]	61	VI	29.34±0.10	27	···	···	27	24.88±0.11	15	···	···	···	···
Coma Cluster													
I4051	···	···	···	···	···	···	···	···	···	V=27.72:±0.35	16	···	···
N4881	···	···	···	···	···	···	···	···	···	···	···	F814W=33.64:±0.29	7
NGC 7331 Group													
N7331	13	VI	30.89±0.10	28	···	···	···	···	···	···	···	I =28.90±0.14	1
N7457	···	···	···	···	···	···	···	···	···	···	···	I=28.76±0.20	1
	···	···	···	···	···	···	···	···	···	···	···	F814W=29.12±0.05	2
Other													
IC4182	28	VI	28.36±0.08[u]	20	···	···	···	···	···	···	···	···	···
N300	16	BVRI	26.66±0.10	29	···	···	34	22.40±0.40[r]	16	···	···	···	···
N2090	35	VI	30.45±0.08	30	···	···	···	···	···	···	···	···	···
N2541	27	VI	30.47±0.08	31	···	···	···	···	···	···	···	···	···
N3115	···	···	···	···	26.21±0.29[s]	26	52	25.72±0.17	17	V =22.45±0.08	17	I =28.43±0.06	1
N3115DW1	···	···	···	···	···	···	···	···	···	V =23.1±0.8	18	···	···
N3621	36	VI	29.13±0.11	32	···	···	···	···	···	···	···	···	···
N4365	···	···	···	···	···	···	···	···	···	B =25.38±0.46	14	I =30.18±0.14	1
	···	···	···	···	···	···	···	···	···	V =24.27±0.30	19	K_s=25.14±0.11	5
	···	···	···	···	···	···	···	···	···	···	···	K'=26.09±0.11	3
N4373	···	···	···	···	···	···	···	···	···	···	···	I =31.59±0.15	1
	···	···	···	···	···	···	···	···	···	···	···	$F814W$ =31.46±0.05	4
N4594	···	···	···	···	···	···	204	25.36±0.08	18	···	···	I =28.42±0.10	1
	···	···	···	···	···	···	···	···	···	···	···	F814W=28.71±0.11	2
N4603	···	···	···	···	···	···	···	···	···	···	···	···	···
N5170	···	···	···	···	···	···	···	···	···	V =24.16±0.23	20	···	···
N5481	···	···	···	···	···	···	···	···	···	V =24.3±0.5	21	···	···
N5846	···	···	···	···	···	···	···	···	···	V =25.19±0.12	22	I =30.70±0.19	1
N708	···	···	···	···	···	···	···	···	···	···	···	$F814W$ =33.24±0.15	8
N5193	···	···	···	···	···	···	···	···	···	···	···	$F814W$ =32.24±0.10	8
IC4296	···	···	···	···	···	···	···	···	···	···	···	$F814W$ =32.38±0.08	8
N7014	···	···	···	···	···	···	···	···	···	···	···	$F814W$ =32.97±0.08	8

Table 3—Continued

		Cepheids			TRGB			PNLF		GCLF		SBF	
Galaxy	No[a]	Bands	$(m-M)\pm\sigma$ [b]	Ref[c]	$I_{TRGB}\pm\sigma$ [d]	Ref [e]	No[f]	$m^*_{5007}\pm\sigma$ [g]	Ref [h]	$m_T\pm\sigma$ [i]	Ref [j]	$\overline{m}\pm\sigma$ [k]	Ref [l]

[a]Number of Cepheids used in fitting the PL relation.

[b]Cepheid distance modulus. Distance moduli followed by a colon are not considered reliable for the reasons described in §3. The Cepheid PL relation is calibrated assuming a distance modulus and reddening to the LMC $\mu = 18.50 \pm 0.13$ mag and $E(B-V) = 0.10$ mag respectively. This calibration is common to all Cepheid distances reported here. Furthermore, all fits to the PL data are performed by fixing the slope of the relation to the values determined for the calibrating LMC sample. All Cepheid distances are scaled adopting a ratio of total to selective absorption $R_V = 3.3$ mag. See Ferrarese et al. (1999) for further details. The error on the distance moduli are random to the collective sample of Cepheids. Systematic errors amount to 0.16 mag for the galaxies observed with the *HST*, and 0.13 mag for the ground based galaxies.

[c]References for the Cepheid Distances: 1. Tolstoy et al. (1995a); 2. Sakai, Madore & Freedman (1999); 3. Madore & Freedman (1991); 4. Freedman, Wilson, & Madore (1991); 5. This paper, data from Musella, Piotto & Capaccioli (1997); 6. Gallart, Aparicio & Vilchez (1996); 7. Sakai, Madore & Freedman (1996); 8. Sakai, Madore & Freedman (1997); 9. This paper, with data from Welch et al. (1987); 10. Silbermann et al. (1996); 11. Prosser et al. (1999); 12. Silbermann et al. (1999); 13. Mould et al. (1999); 14. Tolstoy et al. (1995b); 15. Freedman et al. (1994); 16. Hoessel, Saha & Danielson (1998). 17. Kelson (1999); 18. Sakai et al. (1999); 19. Graham et al. (1997); 20. Gibson et al. (1999), for NGC 4496A, NGC 5253, NGC 4536, IC 4182 and NGC 4639, the data is also described in Saha et al. (1994, 1995, 1996a, 1996b, 1997, 1999); 21. Turner et al. (1998); 22. Gibson et al. (1998); 23. Ferrarese et al. (1996); 24. Graham et al. (1998); 25. Pierce et al. (1994); 26. Macri et al. (1999); 27. Kelson (1996); 28. Hughes (1998); 28. Freedman et al. (1992); 30. Phelps et al. (1998); 31. Ferrarese et al. (1998); 32. Rawson et al. (1997);

[d]I magnitude for the tip of the RGB. The magnitudes are not corrected for either internal or Galactic extinction.

[e]References for the TRGB Distances: 1. Armandroff et al. (1998); 2. Hopp et al. (1999); 3. Grebel & Guhathakurta (1998); 4. Lee & Byun (1999); 5. Sakai, Madore & Freedman (1998); 6. Freedman (1988); 7. Caputo et al. (1999); 8. Tolstoy et al. (1998); 9. Lee (1995a); 10. Lee (1995b); 11. Reid, Mould & Thompson (1987); 12. Mould, Kristian & da Costa (1984); 13. Mould & Kristian (1986); 14. Lee (1993); 15. Minniti et al. (1999); 16. Gallart, Aparicio & Vilchez (1996); 17. Sakai, Madore & Freedman (1996); 18. Sakai, Madore & Freedman (1997); 19. Lee, Freedman, & Madore (1993); 20. Caldwell et al. (1998); 21. Sakai & Madore (1999); 22. Sakai et al. (1997); 23. Harris et al. (1998); 24. Ferguson, Tanvir & Hippel (1998); 25. Soria et al. (1996); 26. Elson (1997).

[f]Number of Planetary Nebulae used in fitting the PNLF. This excludes PNe that are fainter than the completeness limit adopted for the data.

[g]Apparent cutoff λ5007 magnitude for the PNLF. Magnitudes are not corrected for extinction, either internal or Galactic. Magnitudes followed by a colon are not considered reliable for the reasons described in §3.

[h]References for the PNLF m^*_{5007} cutoff magnitudes: 1. Jacoby, Walker & Ciardullo (1990); 2. Ciardullo et al. (1989); 3. Richer & McCall (1992); 4. Ciardullo, Jacoby & Harris (1991); 5. McMillan, Ciardullo & Jacoby (1993); 6. Jacoby et al. (1989); 7. Feldmeier, Ciardullo & Jacoby (1997); 8. Ciardullo, Jacoby & Ford (1989); 9. Jacoby, Ciardullo & Harris (1996); 10. Jacoby, Ciardullo & Ford (1990); 11. Ciardullo et al. (1998); 12. McMillan, Ciardullo & Jacoby (1994); 13. Hui et al. (1993); 14. Phillips et al. (1992); 15. Feldmeier, Ciardullo & Jacoby (1996); 16. Soffner et al. (1996); 17. Ciardullo, Jacoby& Tonry (1993); 18. Ford et al. (1996).

[i]The apparent $V-$band magnitude of the turnover of the globular cluster luminosity function, uncorrected for reddening.

[j]References for the GCLF Distances: 1. Reed, Harris & Harris (1994); 2. Blakeslee & Tonry (1996); 3. Elson et al. (1998); 4. Della Valle et al. (1998); 5. Ostrov, Forte & Geisler (1998); 6. Grillmair et al. (1999); 7. Richtler et al. (1992); 8. This paper, data from Perelmuter & Racine (1995); 9. Pritchet & van den Bergh (1985); 10. Forbes (1996a); 11. Fleming et al. (1995); 12. Neilsen, Tsvetanov & Ford (1997); 13. Kundu et al. (1999); 14. Harris et al. (1991); 15. Lee, Kim & Geisler (1998); 16. Baum et al. (1996); 17. Kundu & Whitmore (1998); 18. Durrell et al. (1996); 19. Forbes (1996b); 20. Fischer et al. (1990); 21. Madejsky & Rabolli (1995); 22. Forbes, Brodie & Huchra (1996).

[k]SBF magnitudes. All values are not corrected for extinction. The I-SBF fluctuation magnitudes reported here must be cited as Ajhar et al. (1999).

[l]References for the SBF Distances: 1. Ajhar et al. (1999); 2. Ajhar et al. (1997); 3. Jensen, Tonry & Luppino (1998); 4. Pahre et al. (1999); 5. Pahre & Mould (1994); 6. Neilsen, Tsvetanov & Ford (1997), not used for distance determinations since the galaxy's mean color is not given.; 7. Thomsen et al. (1997); 8. Lauer et al. (1998).

[m]Adopted zero point for the Cepheid PL relations.

[n]The distance modulus is determined as an upper limit from the magnitude of the brightest PN in a sample of only seven objects.

[o]The published value is $T_1 = 23.0 \pm 0.15$. The $C - T_1$ color is also available, allowing to convert the T_1 magnitude to V using the formulas by Geisler (1996)

[p]The published value is $T_1 = R = 23.3 \pm 0.1$. The $C - T_1$ color is also available, allowing to convert the T_1 magnitude to V using the

formulas by Geisler (1996)

[q]For the distance to M101, we adopt the value derived by Kelson et al. (1996). Stetson et al. (1998) also derived a distance to M101 based on HST/WFPC2 observations of a different field of the galaxy.

[r]Distance modulus determined using the cumulative PNLF.

[s]The quoted values is calculated from the published unreddened values using $A_I = 0.05$.

[t]These distances have been modified from the published value to account for period incompleteness bias (see §3 and Table 4 for further details).

[u]Distances from Gibson's et al. (1999), on the Hill et al. (1998) zero point (from column 2 of Table 4 of Gibson et al. 1999).